Thermal Stability of Hydrazinium Nitroformate (HNF) Assessed by Heat Generation Rate and Heat Generation and Mass Loss

Manfred A. Bohn
Fraunhofer-Institut für Chemische Technologie (ICT), Postfach 1240, D-76318 Pfinztal-Berghausen, Germany
Email: Manfred.Bohn@ict.fraunhofer.de

Abstract: *HNF, hydrazinium nitroformate, $H_3NNH_2^+ \cdot C(NO_2)^{3-}$, is a water soluble salt. It has a positive oxygen balance of 13%, a much more positive enthalpy of formation than ammonium perchlorate (AP) and a much higher heat of explosion than AP, 5579 J g^{-1} against 1972 J g^{-1}. Additionally it has no chlorine and all the problems with hydrogen chloride formation can be avoided when used as oxidizer in rocket propellant formulations. All these advantages together could make HNF an oxidizer with better performance than AP. One inherent disadvantage may be the lesser thermal stability of HNF. Therefore an extensive investigation was performed on the thermo-chemical stability of HNF. Three sample lots of HNF have been investigated at ICT. They were provided by APP BV, The Netherlands. The thermal stability was determined by the following methods:*

- *autoignition temperature with 0.2 g at 5 °C min^{-1} heat rate in a Wood's metal bath*
- *vacuum stability test (VST)*
- *heat generation rate as function of time and temperature*
- *mass loss as function of time and temperature*
- *adiabatic self heat rate.*

Lots 2 and 3 have been characterised by heat generation rate at 60 °C, 65 °C, 70 °C and 75 °C and in short by mass loss. Lot 1 was extensively used for mass loss determinations in the temperature range 50 to 80 °C. HNF shows high heat generation rates. All curves from both methods indicate self accelerating behaviour. They have been described with autocatalytic reaction kinetic models. The Arrhenius parameters have been determined for lot 1 from mass loss data and for lots 2 and 3 from heat generation data. The activation energies for the intrinsic decomposition reaction are 166, 139 and 132 kJ mol^{-1} and for the autocatalytic reaction 159, 128 and 117 kJ mol^{-1} in the order lots 1, 2, 3. The kinetic data are compared and discussed. Data for lifetime at different temperatures are given in terms of the times to reach preset values of mass loss and energy loss.

Keywords: *autocatalytic, kinetic, HNF*

Introduction

The chemical formula of HNF is shown in Figure 1. It is a salt between the nitroform acid and hydrazine. One may name the substance as hydrazinium trinitromethanate and by ignoring its salt character hydrazine trinitromethane. It is easily soluble in water. Especially at elevated temperatures the salt may be in an equilibrium state with its pre-dissociated form, shown in Figure 2, as is assumed also for ammonium nitrate (AN) and ammonium dinitramide (ADN). In Table 1 some data are compiled to characterize and compare HNF with other oxidizers.

HNF has been investigated by thermal analysis several times already.[2–4] These papers concentrate

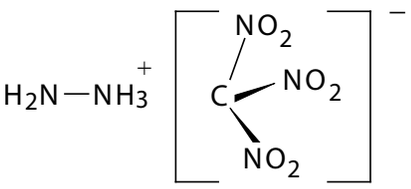

Figure 1. *Chemical formula of HNF, hydrazinium nitroformate.*

Table 1. *Performance data of the oxidizers ADN, AP, AN and HNF. The values of the heats of explosion and gas volumes have been calculated by the ICT-Thermodynamic-Code. The other data are from the ICT-Thermochemical Data Base*[1]

Substance	Molar mass/ g mol^{-1}	O_2 balance (%)	Enthalpy of formation ΔH_f^0/		Q_{EX}[a]/ J g^{-1}	Density/ g cm^{-3}	Gas vol[b]/ cm^3 g^{-1}	T_M[c]/°C
			kJ mol^{-1}	J g^{-1}				
ADN	124.056	+25.8	−149.8	−1207.5	3337	1.81	592	92.9
AP	117.489	+34.0	−295.8	−2517.7	1972	1.95	533	130; D
AN	80.043	+20.0	−365.6	−4567.5	2479	1.73	459	169.9
HNF	183.081	+13.1	−76.9	−420.0	5579	1.91	568	124; D

[a] Q_{EX} heat of explosion, value with reaction water as liquid (25 °C). [b] Gas volume at 25 °C, 1 bar without water, for thermodynamically controlled combustion. [c] D in the column of T_M (melting temp.) means decomposition at the given temperature, which may vary with the sensitivity of the observation.

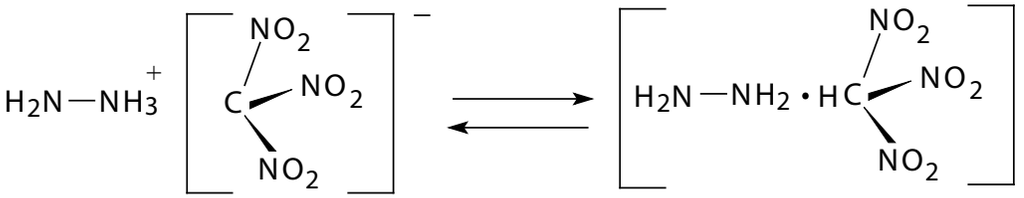

Figure 2. *Equilibrium between salt form and pre-dissociated form.*

mainly on decomposition products, decomposition mechanisms and safety aspects. In some data[5] on activation energies for the decomposition of HNF, measurements (TGA, DSC) are given obtained by TA, and typical TA data evaluation was performed. These TA models do not describe the data well. The activation energies given[5] are in the range of 217 and 235 kJ mol obtained by thermal analysis (TA). In the present paper the data measured between 50 and 80 °C have been described with autocatalytic models, which give very good reproductions of the isothermal measurement curves.

Substances, measurement methods and conditions

Three lots of HNF were shipped to ICT from the company APP (Aerospace Propulsion Products BV), RT Klundert, The Netherlands. The colour of all three samples was intensely yellow-orange. All lots were of type S according to the APP classification. The particle shape was different between HNF lots 1/2 and HNF lot 3. HNF lots 1/2 were more needle-like and coarser than HNF lot 3, which appeared nearly equal in all three geometric dimensions. The mean particle size of lot 1 was about 240 µm with a length to diameter ratio of 7.4, and for lot 3 these were found to be 76 µm and 2.8. Table 2 lists some data. The HNF was used as delivered. The purity is, according to APP information, between 98.8 mass% and 99.6 mass% based on acid content (not further specified) and between 97.2 mass% and 99.6 mass% based on hydrazine content. To determine the thermal stability, several test methods and measuring methods were applied:

- autoignition temperature at 5 °C min^{-1} heat rate, 200 mg sample size;
- vacuum stability test (VST), 2 g sample size;
- heat generation rate (HGR, dQ/dt) as a function of time and temperature, determined with a TAM^{TM} (Thermal Activity Monitor), produced by Thermometric AB, Sweden; 3 ml ampoules, sample amount between 1.2 and 1.4 g;

  HNF lot 1 75 °C

Table 2. *Characteristic data determined with HNF lot 1. Experimental oxygen content as difference to 100 mass% from measured CNH data. S means limit energy for impact (impact sensitivity); R means limit force for friction (friction sensitivity)*

	Elemental composition [mass%]				*S*/Nm	*R*/N	Density/ g cm^{-3}	Heat of comb/J g^{-1}
	C	H	N	O				
Measured at ICT	7.01	2.78	37.64	(52.57)	2	16	1.846	5796
Theoretical values	6.560	2.753	38.254	52.433	—	—	1.87–1.93	(5579)
APP-data[6,7]	—	—	—	—	2–5	18–36	1.86	5824

HNF lot 2 60 °C, 65 °C, 70 °C, 75 °C

HNF lot 3 60 °C, 65 °C, 70 °C, 75 °C

- mass loss (ML) as function of time and temperature, determined in PID controlled and isothermally operated aluminium block ovens, sample amount 1 g and 2 g per glass;

  HNF lot 1 50 °C, 60 °C, 65 °C, 70 °C, 75 °C, 80 °C

  HNF lot 2 65 °C, 70 °C, 75 °C

  HNF lot 3 65 °C, 70 °C, 75 °C

- adiabatic self heat rate, determined with an ARC™ (Accelerating Rate Calorimeter), 200 mg sample amount;

With these methods two tests on the samples are achieved:

- gas generation by VST and mass loss
- net effect of the sum of heats of reactions during decomposition by autoignition temperature, heat generation rate, adiabatic self heating.

These different investigations into the decomposition behaviour of a sample confirms the results, if they are consistent.[8]

Results

Stability tests

The autoignition temperature was determined with a standardized apparature at 5 °C min^{-1} heat rate in a Wood's metal bath. A sample mass of 0.2 g was used in special vials. The vacuum stability test, also a standardized test, was performed with the special conditions adapted to HNF by TNO-PML: test temperature 60 °C, test time 48 h. The sample amount was 2 g. The gas generation was determined in the vacuum apparatus with an integrated mercury column manometer. The last two columns of Table 3 show the values transformed from 60 °C, 48 h to the standard conditions of 90 °C, 40 h and 100 °C, 40 h, whereby a factor of 4 for a 10 °C temperature change has to be used because of the values of activation energy found. The limiting value of gas generation volume under standard conditions is 1.2 ml g^{-1} for both test conditions for the assessment 'stable'. Even at 90 °C this limit is far exceeded. For 80 °C no official test condition exists. Scaling the 90 °C conditions to 80 °C results in a limiting value of 0.3 ml g^{-1}.

Heat generation rate and heat generation

Measurement data

The heat generation rate (HGR, dQ/dt) was measured with a TAM™ microcalorimeter in the standard glass ampoules. Because HNF has a high positive oxygen balance one may assume that

Table 3. *Stability test data.*

HNF lot	Autoignition temp./ °C at 5 °C min^{-1}	VST [ml g^{-1}] 60 °C, 48 h, 2 g	Extrapolated [ml g^{-1}] 80 °C, 40h	Extrapolated [ml g^{-1}] 90 °C, 40 h	Extrapolated [ml g^{-1}] 100°C, 40 h
HNF lot 1	131	0.082	1.10	4.4	17.5
HNF lot 2	129	0.084	1.13	4.5	17.9
HNF lot 3	129	0.072	0.95	3.8	15.4

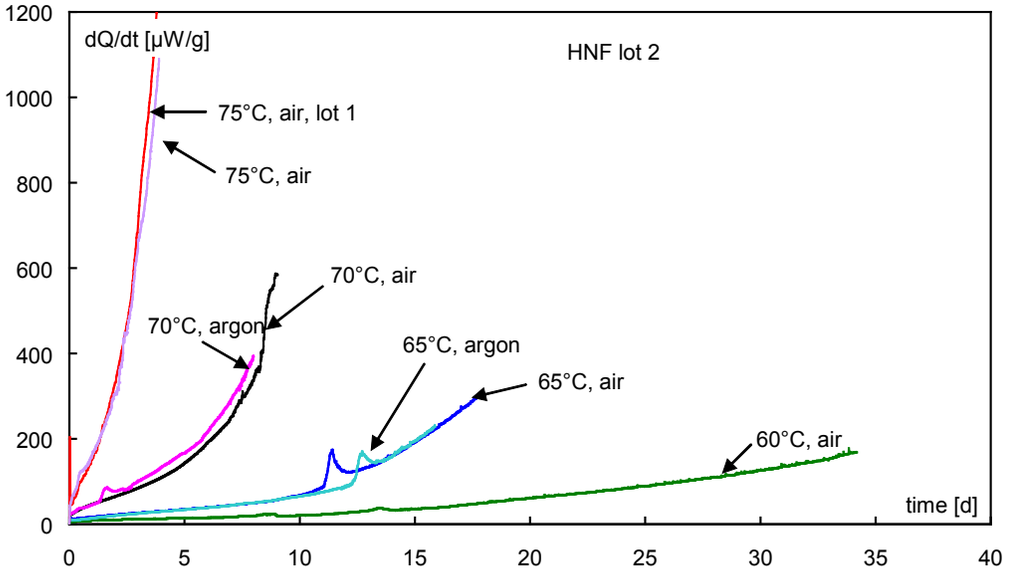

Figure 3. *HNF lot 2. Heat generation rate (HGR) as function of time at temperatures between 60 °C and 75 °C. HNF lot 1 is included for comparison.*

measurements with air inside the ampoule should not greatly influence the HGR. Some measurements were also made in argon atmosphere. This was achieved by closing the ampoules in a high performance glove box from M. Braun Inertgas-Systeme GmbH, D-85748 Garching, Germany, type MB-200–MOD, operated with argon. The comparison of the curves indicates that the assumption is valid, see Figure 3 for lot 2. HNF shows complicated decomposition behaviour after some initial period. This is found in the HGR curves in a significant way. After some time period a sudden acceleration in heat generation activity can be seen, Figure 3, lot 2 and Figure 5, lot 3. After a further period mitigation occurs and the curve again has a more smooth shape, but

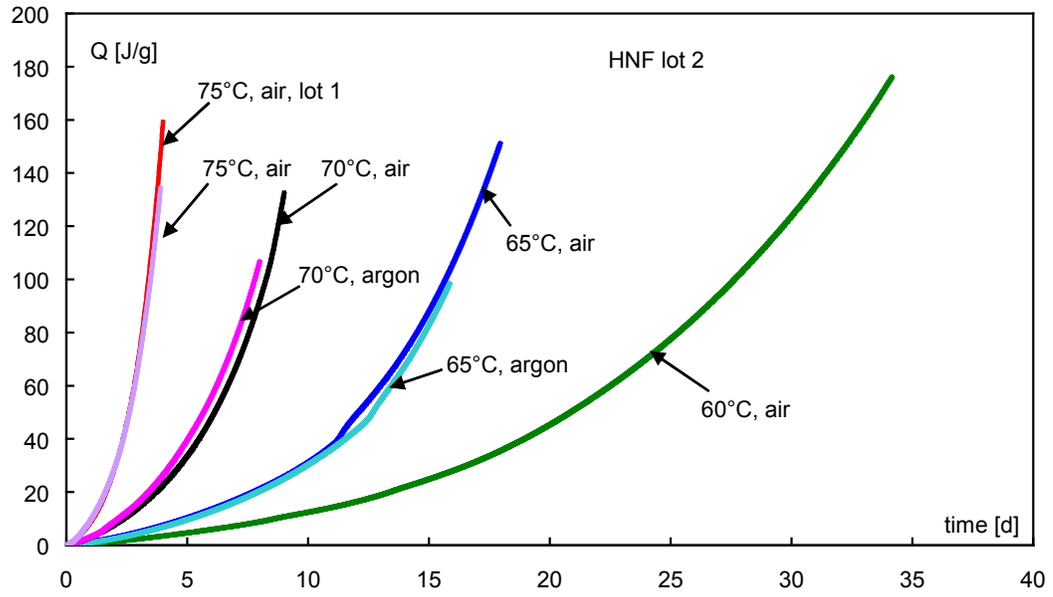

Figure 4. *HNF lot 2. Heat generation (HG) as function of time between 60 °C and 75 °C. HNF lot 1 is included for comparison.*

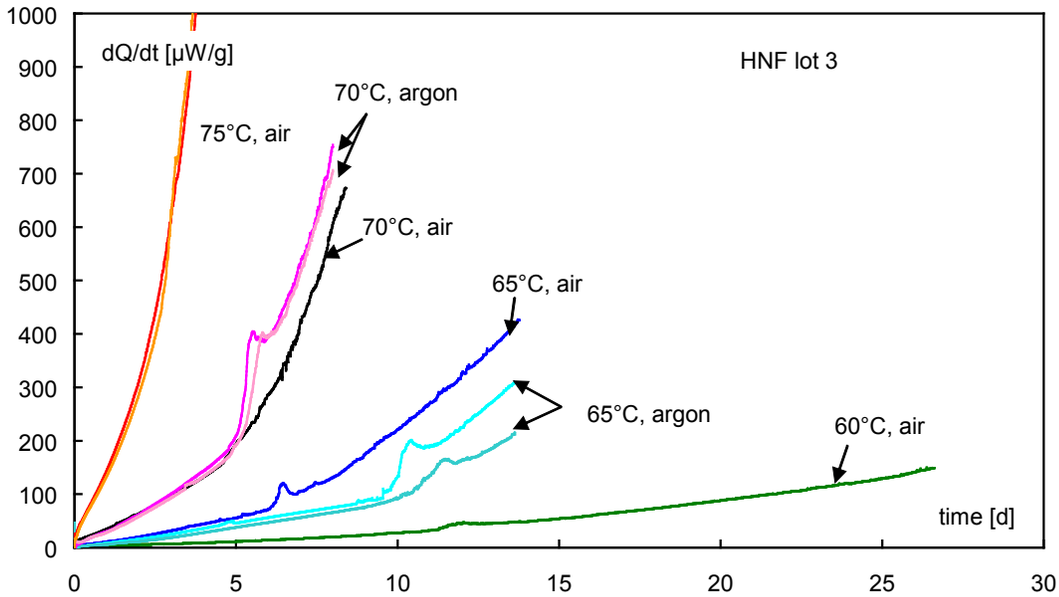

Figure 5. *HNF lot 3. Heat generation rate (HGR) as function of time between 60 °C and 75 °C. The change of the atmosphere gives no consistent picture with lot 3.*

the HGR values then increase more rapidly. The interpretation is that the intermediate activity has produced further autocatalytically effective species or at least raised their concentration peakwise. This effect can be seen especially at temperatures causing a medium decomposition rate, mainly at 65 °C and 70 °C. But close inspection of the curves at 60 °C reveals this effect also. At 75 °C the decomposition rate is already so high that the described activity increase is flattened and hard to see. Remarkable are the very high values of the measured heat generation rates compared with values of a double base propellant, which range between 15 and 60 µW g^{-1} at 75 °C. Figures 4 and 6 show the heat generation of the two HNF lots. Figure 7 compares lots 2 and 3 via heat generation (HG, Q). HNF lot 3 is, during the initial conversion period, always somewhat more stable than HNF

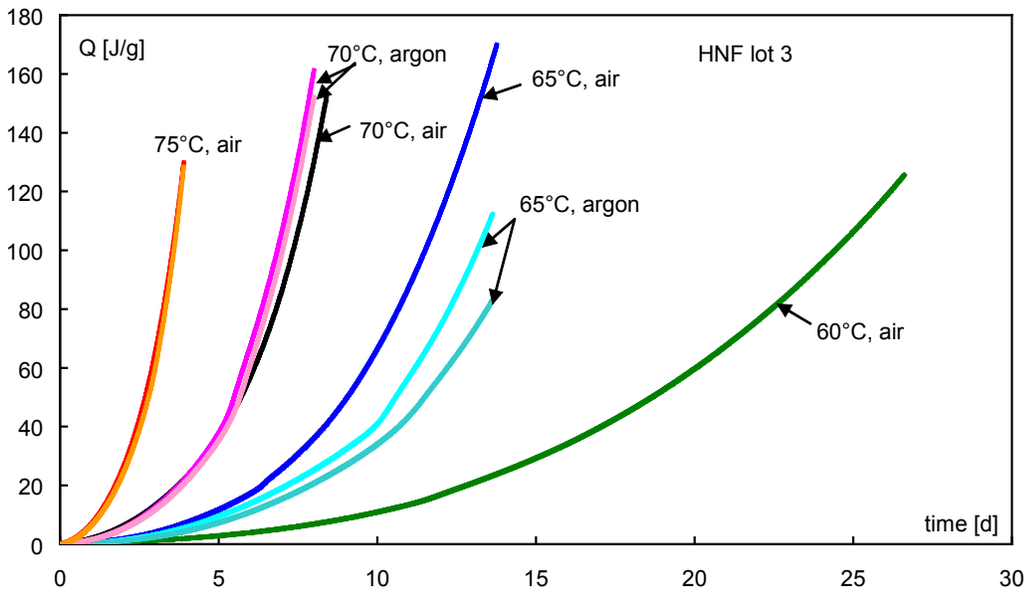

Figure 6. *HNF lot 3. Heat generation (HG) as function of time between 60 °C and 75 °C.*

$$\left(\frac{dQ_A(t,T)}{dt}\right)\Big|_T = -\left(\frac{\mathrm{d}A(t,T)}{\mathrm{d}t}\right)\Big|_T \cdot\left(-\Delta H_{\mathrm{R,A}}\right) = -\left(\frac{\mathrm{d}M_{\mathrm{A}}(t,T)}{\mathrm{d}t}\right)\Big|_T \cdot\frac{1}{m_{\mathrm{A}}}\cdot\left(-\Delta H_{\mathrm{R,A}}\right) \quad (1)$$

$$Q_{\mathrm{A}}(t_{\mathrm{e}}) = (-\Delta H_{\mathrm{RA}})\cdot A(0) \quad (2)$$

$$\begin{cases} \left(\frac{\mathrm{d}Q_{\mathrm{Ar}}(t,T)}{\mathrm{d}t}\right)\Big|_T = -\left(\frac{\mathrm{d}A_{\mathrm{r}}(t,T)}{\mathrm{d}t}\right)\Big|_T = -\left(\frac{\mathrm{d}M_{\mathrm{Ar}}(t,T)}{\mathrm{d}t}\right)\Big|_T \\ Q_{\mathrm{Ar}}(t,T) = Q_{\mathrm{A}}(t,T)/Q_{\mathrm{A}}(t_{\mathrm{e}}); \quad A_{\mathrm{r}}(t,T) = A(t,T)/A(0); \quad M_{\mathrm{Ar}}(t,T) = M_{\mathrm{A}}(t,T)/M_{\mathrm{A}}(0) \end{cases} \quad (3)$$

$$\mathrm{A} + \mathrm{B} \xrightarrow{k_2} 2\mathrm{B} + \mathrm{C} + \mathrm{S}\ \ (-\Delta H_{\mathrm{R},2}) \qquad \mathrm{A} \xrightarrow{k_1} \mathrm{B} + \mathrm{C} + \mathrm{S}\ \ (-\Delta H_{\mathrm{R},1}) \quad (4)$$

intrinsic decomposition — autocatalytic decomposition

lot 2 but then this changes and HNF lot 3 becomes significantly the more unstable substance with higher decomposition rates. At temperatures above 70 °C the difference diminishes because of the already very high decomposition rates. Because of the high HGR and high gas generation rates the probability of the glass ampoule breaking is high.

Evaluation of heat generation data

Equation (1) shows the connection between the quantities heat generation rate $\mathrm{d}Q_{\mathrm{A}}/\mathrm{d}t$, molar amount changing rate $\mathrm{d}A/\mathrm{d}t$ and mass changing rate $\mathrm{d}M_{\mathrm{A}}/\mathrm{d}t$ of decomposing substance A. With Equation (2) the total amount of evolved heat $Q_{\mathrm{A}}(t_{\mathrm{e}})$ by the complete decomposition of A is given, using the molar heat of reaction $(-\Delta H_{\mathrm{R,A}})$. The complete decomposition of A is achieved at infinite time according to a first order reaction. This is not a real world property and the time t_{e} is introduced, at which the decomposition of A is no longer measurable. The reaction kinetic determined quantity $Q_{\mathrm{A}}(t_{\mathrm{e}})$ is often not obtainable because the measurements may take too long a time or the suitable apparatus is not available. As reference

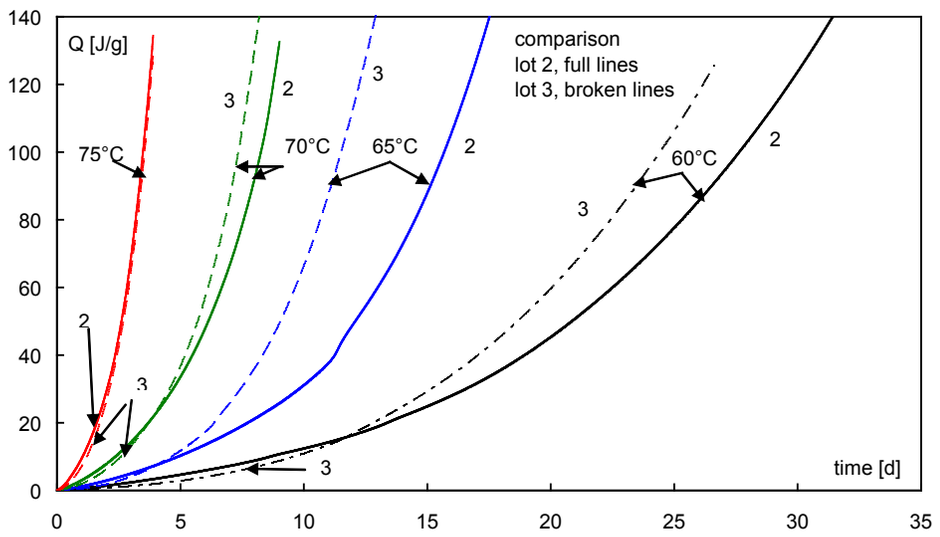

Figure 7. *Comparison of HNF lot 2 and HNF lot 3. Heat generation (HG) as function of time at temperatures between 60 °C and 75 °C.*

$$\left(\frac{\mathrm{d}A(t,T)}{\mathrm{d}t}\right)\Bigg|_T = -k_1(T)\cdot A(t,T) - k_2(T)\cdot A(t,T)\cdot B(t,T) \tag{5}$$

$$\left(\frac{\mathrm{d}Q_A(t,T)}{\mathrm{d}t}\right)\Bigg|_T = +k_1(T)\cdot(-\Delta H_{\mathrm{R},1})\cdot A(t,T) + k_2(T)\cdot(-\Delta H_{\mathrm{R},2})\cdot A(t,T)\cdot B(t,T) \tag{6}$$

$$\left(\frac{\mathrm{d}Q_{\mathrm{Ar}}(t,T)}{\mathrm{d}t}\right)\Bigg|_T = k_Q^1(T)\cdot\left(1-Q_{\mathrm{Ar}}(t,T)\right) + k_Q^2(T)\cdot\left(1-Q_{\mathrm{Ar}}(t,T)\right)\cdot\left(F+Q_{\mathrm{Ar}}(t,T)\right) \tag{7}$$

$$(-\Delta H_{\mathrm{R,A}}) = (\Delta H_{\mathrm{R},1}) = (\Delta H_{\mathrm{R},2}) \tag{8}$$

$$k_Q^1(T) = k_{\mathrm{ML}}^1(T) = k_{\mathrm{A}}^1(T) = k_1(T) \qquad k_Q^2(T) = k_{\mathrm{ML}}^2(T) = k_{\mathrm{A}}^2(T) = k_2(T)\cdot A(0) \tag{9}$$

$$\begin{cases} Q_{\mathrm{A}}(t,T) = OF_Q + Q_{\mathrm{A}}(te)\cdot\left(1-\dfrac{k_{\mathrm{A}}^1(T)+k_{\mathrm{A}}^2(T)}{k_{\mathrm{A}}^2(T)+k_{\mathrm{A}}^1(T)\cdot\exp\left(\left(k_{\mathrm{A}}^1(T)+k_{\mathrm{A}}^2(T)\right)\cdot t\right)}\right) \\ Q_{\mathrm{A}}(t,T) = OF_Q + Q_{\mathrm{A}}(t_e)\cdot\left(1-\dfrac{k_{\mathrm{A}}^1(T)+\left(F+1\right)\cdot k_{\mathrm{A}}^2(T)}{k_{\mathrm{A}}^2(T)+\left(k_{\mathrm{A}}^1(T)+F\cdot k_{\mathrm{A}}^2(T)\right)\cdot\exp\left(\left(k_{\mathrm{A}}^1(T)+\left(F+1\right)\cdot k_{\mathrm{A}}^2(T)\right)\cdot t\right)}\right) \end{cases} \tag{10}$$

$$\begin{cases} \left(\dfrac{\mathrm{d}Q_{\mathrm{A}}(t,T)}{\mathrm{d}t}\right)\Bigg|_T = Q_{\mathrm{A}}(t_{\mathrm{e}})\cdot\Bigg((k_Q^1(T)\cdot\dfrac{\left(k_{\mathrm{A}}^1(T)+k_{\mathrm{A}}^2(T)\right)}{k_{\mathrm{A}}^2(T)+k_{\mathrm{A}}^1(T)\cdot\exp\left(\left(k_{\mathrm{A}}^1(T)+k_{\mathrm{A}}^2(T)\right)\cdot t\right)} \\ \qquad + k_Q^2(T)\cdot\dfrac{\left(k_{\mathrm{A}}^1(T)+\cdot k_{\mathrm{A}}^2(T)\right)}{k_{\mathrm{A}}^2(T)+k_{\mathrm{A}}^1(T)\cdot\exp\left(\left(k_{\mathrm{A}}^1(T)+k_{\mathrm{A}}^2(T)\right)\cdot t\right)}\cdot \\ \qquad \cdot\left(1-\dfrac{\left(k_{\mathrm{A}}^1(T)+k_{\mathrm{A}}^2(T)\right)}{k_{\mathrm{A}}^2(T)+k_{\mathrm{A}}^1(T)\cdot\exp\left(\left(k_{\mathrm{A}}^1(T)+k_{\mathrm{A}}^2(T)\right)\cdot t\right)}\right)\Bigg) \end{cases} \tag{11}$$

quantity the heat of explosion $Q_{\mathrm{EX,A}}$ is taken therefore, with the value from the thermodynamic calculation.[1] Equation (3) is the normalized form of equation (1) using the normalizations also given in equation (3).

The data evaluation was done with reaction kinetic modelling described in detail already elsewhere.[9] Here the important relations are given in short. HNF decomposes autocatalytically. The corresponding reaction scheme is shown in equation (4). Substance A decomposes into gases C, solids S and into an autocatalytically effective product B. In the second parallel reaction B reacts with A and accelerates its consumption as shown in equation (4).

The intrinsic decomposition of A cannot be suppressed by stabilizers with their common function. To use stabilizers for this purpose would

require the 1:1 addition of a substance which is able to stabilize the electronic system of HNF by complex formation. With stabilizers of common function only the autocatalytic reaction can be influenced by removing B by chemically bonding it to the stabilizing substance. In equation (5) the intrinsic or inherent decomposition of A is included as a first order reaction. Reformulation to heat generation rates leads to equation (6).[9]

Equation (6) is transformed into equation (7) used here by normalization with $Q_{ref} = Q_A(t_e)$. B(0) must not be zero. This is considered in equation (7) by the factor F = B(0)/A(0). The effect of $F \neq 0$ is to emphasize the autocatalytic channel. This can change the course of the measured curve strongly.[9] In the following F is set to zero here. If the two heats of reaction in equation (4) are set equal then, with equations (8) and (9), equation (10) results. The equation used here for the modelling of the heat generation is this equation (10) with $F = 0$ as argued above. For completeness the corresponding equation is given with $F \neq 0$ in equation (10). It is named model 'Q: first order + autocatalytic'. To calculate the heat generation rate with the reaction rate constants obtained, equation (11) is used. Notice the equivalence of the rate constants with different indexing, see equation (9).

To calculate the times $t_{yEL,A}$ to reach a certain energy loss EL by decomposition in substance A equation (12) is used in the case of autocatalytic decomposition. For completeness both versions are given, for $F = 0$ and $F \neq 0$. The corresponding quantities are explained as follows.

$Q_{A,ref} = Q_A(t_e,T)$ is maximum energy of the sample (here $Q_A(t_e) = Q_{EX,A} = 5580$ J g^{-1})

$Q_A(t_{yQ,A}(T))$ is amount of energy released by the sample A

$Q_A(t_e,T) - Q_A(t_{yQ,A}(T))$ is momentary energy content of the sample A

$y_{Q,A} = (Q_A(t_e,T) - Q_A(t_{yQ,A}(T))) / Q_{A,ref}$

$t_{yEL,A}(T)$ is the time to reach $y_{EL,A} = 100\% \cdot (1 - y_{Q,A})$; $t_{yEL,A} = t_{yQ,A}$

If only a first order decomposition reaction is active, equation (13) applies to calculate the times $t_{yEL,A}$. A smaller $Q_{EX,A}$ value does not change the $E_{aQ,i}$ values; it changes $Z_{Q,i}$.

Figure 8 shows an example of the modelling of heat generation with HNF lot 2. The obtained reaction rate constants are compiled in Tables 4 and 5 for lots 2 and 3, together with the Arrhenius parameters. The corresponding Arrhenius plots can be seen in Figures 9 and 10 for HNF lot 2 and Figures 11 and 12 for HNF lot 3. The Arrhenius parameters are given for measurements in air only and for the combined measured data 'air + argon'. Again the description of the data with the model is very good as can be seen from the correlation coefficients for the individual temperatures.

$$\begin{cases} t_{y_{EL,A}}(T) = \dfrac{1}{k_A^1(T) + k_A^2(T)} \cdot \ln\left(\dfrac{\dfrac{1}{y_{Q,A}} \cdot \left(k_A^1(T) + k_A^2(T) \right) - k_A^2(T)}{k_A^1(T)} \right) \\ t_{y_{EL,A}}(T) = \dfrac{1}{k_A^1(T) + (F+1) \cdot k_A^2(T)} \cdot \ln\left(\dfrac{\dfrac{1}{y_{Q,A}} \cdot \left(k_A^1(T) + (F+1) \cdot k_A^2(T) \right) - k_A^2(T)}{k_A^1(T) + F \cdot k_A^2(T)} \right) \end{cases} \quad (12)$$

$$t_{y_{EL,A}}(T) = \frac{1}{k_A^1(T)} \cdot \ln\left(\frac{1}{y_{Q,A}} \right) \quad (13)$$

for first order decomposition only.

Table 4. *HNF lot 1 and lot 2. Reaction rate constants from autocatalytic modelling of heat generation HG, with $Q_{ref} = Q_{EX} = 5580$ J g^{-1}, air and argon atmosphere*

Temp./°C	$k_{Q,1}$ [1/d]	$k_{Q,2}$ [1/d]	R^2	Atmosphere	Lot
60	$1.4627 \times 10^{-4} \pm 1.8 \times 10^{-7}$	$9.0094 \times 10^{-2} \pm 6.3 \times 10^{-5}$	0.99951	air	2
65	$2.0876 \times 10^{-4} \pm 2.9 \times 10^{-7}$	$1.7909 \times 10^{-1} \pm 1.3 \times 10^{-4}$	0.99969	air	2
70	$5.2097 \times 10^{-4} \pm 1.1 \times 10^{-6}$	$2.9501 \times 10^{-1} \pm 3.9 \times 10^{-4}$	0.99956	air	2
75	$1.2042 \times 10^{-3} \pm 2.0 \times 10^{-6}$	$7.0375 \times 10^{-1} \pm 7.1 \times 10^{-4}$	0.99989	air	2
75	$1.0887 \times 10^{-3} \pm 3.3 \times 10^{-6}$	$7.7276 \times 10^{-1} \pm 1.2 \times 10^{-3}$	0.99989	air	1
65	$1.9363 \times 10^{-4} \pm 5.7 \times 10^{-7}$	$1.7961 \times 10^{-1} \pm 3.1 \times 10^{-4}$	0.99853	argon	2
70	$6.3628 \times 10^{-4} \pm 1.0 \times 10^{-6}$	$2.8351 \times 10^{-1} \pm 3.5 \times 10^{-4}$	0.99973	argon	2
Arrhenius parameters from measurements in air and argon					
E_{ai}/kJ mol^{-1}	146.2 ± 14	132.4 ± 5			
lg(Z_i [1/d])	18.98 ± 2.2	19.69 ± 1.4			
R^2_i	0.978	0.988			
Arrhenius parameters from measurements in air only					
E_{ai}/kJ mol^{-1}	139.3 ± 18	128.4 ± 10			
lg(Z_i [1/d])	17.94 ± 2.8	19.08 ± 1.6			
R^2_i	0.983	0.994			

Mass loss

Measurement data

Because of the limited amount of substance for HNF lot 1 only mass loss measurements could be performed in the necessary extension. Figures 13 to 17 show the mass loss as function of time for all three lots. Figure 13 gives an overview of the

Table 5. *HNF lot 3. Reaction rate constants from autocatalytic modelling of heat generation HG, with $Q_{ref} = Q_{EX} = 5580$ J g^{-1}, air and argon atmosphere*

Temp./°C	$k_{Q,1}$ [1/d]	$k_{Q,2}$ [1/d]	R^2	Atmosphere
60	$1.2965 \times 10^{-4} \pm 4.4 \times 10^{-7}$	$1.1702 \times 10^{-1} \pm 2.1 \times 10^{-4}$	0.99724	air
60	$1.0634 \times 10^{-4} \pm 1.4 \times 10^{-7}$	$1.2863 \times 10^{-1} \pm 7.9$ E-05	0.99478	air
65	$2.4849 \times 10^{-4} \pm 1.0 \times 10^{-7}$	$2.5756 \times 10^{-1} \pm 4.6 \times 10^{-4}$	0.99835	air
65	$1.6623 \times 10^{-4} \pm 4.5 \times 10^{-7}$	$2.5640 \times 10^{-1} \pm 3.1 \times 10^{-4}$	0.99925	argon
65	$1.5178 \times 10^{-4} \pm 4.2 \times 10^{-7}$	$2.3540 \times 10^{-1} \pm 3.3 \times 10^{-4}$	0.99909	argon
70	$4.2145 \times 10^{-4} \pm 5.7 \times 10^{-7}$	$3.9323 \times 10^{-1} \pm 2.6 \times 10^{-4}$	0.99987	air
70	$3.7576 \times 10^{-4} \pm 1.8 \times 10^{-6}$	$4.5477 \times 10^{-1} \pm 9.2 \times 10^{-4}$	0.99873	argon
70	$3.3413 \times 10^{-4} \pm 1.2 \times 10^{-6}$	$4.6363 \times 10^{-1} \pm 7.0 \times 10^{-4}$	0.99928	argon
75	$8.6541 \times 10^{-4} \pm 2.2 \times 10^{-6}$	$8.0396 \times 10^{-1} \pm 1.1 \times 10^{-3}$	0.99976	air
75	$1.0330 \times 10^{-3} \pm 4.2 \times 10^{-6}$	$7.4789 \times 10^{-1} \pm 1.7 \times 10^{-3}$	0.99936	air
Arrhenius parameters from measurements in air and argon				
E_{ai}/kJ mol^{-1}	134.2 ± 13	117.1 ± 4		
lg(Z_i [1/d])	17.05 ± 1.9	17.46 ± 0.6		
R^2_i	0.967	0.995		
Arrhenius parameters from measurements in air only				
E_{ai}/kJ mol^{-1}	132.4 ± 7	116.6 ± 5		
lg(Z_i [1/d])	16.82 ± 1.1	17.38 ± 0.8		
R^2_i	0.994	0.997		

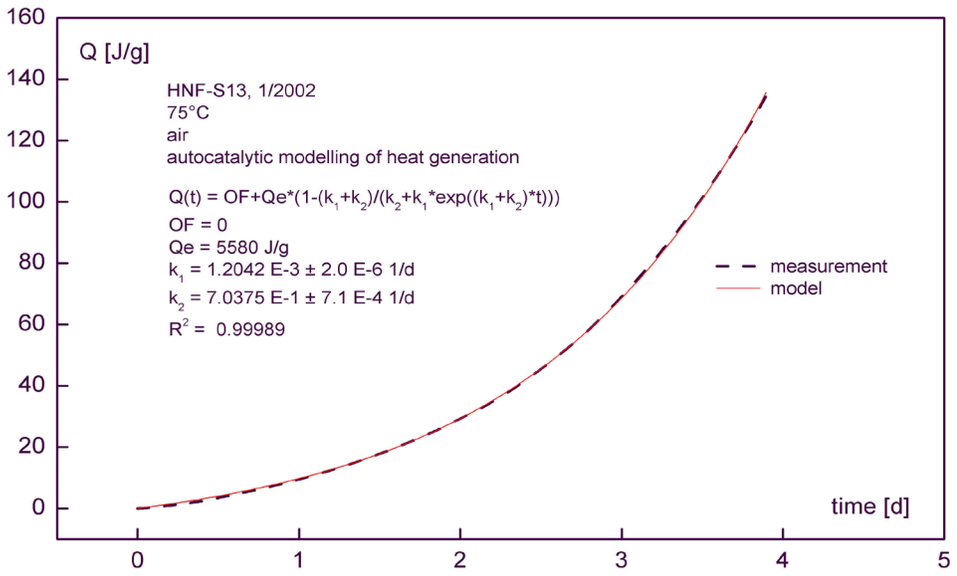

Figure 8. *HNF lot 2: Autocatalytic modelling of the heat generation at 75 °C.*

$$\left(\frac{\mathrm{d}M_{\mathrm{Ar}}(t,T)}{\mathrm{d}t}\right)\Bigg|_{T} = -k^{1}_{\mathrm{ML}}(T)\cdot M_{\mathrm{Ar}}(t,T) - k^{2}_{\mathrm{ML}}(T)\cdot M_{\mathrm{Ar}}(t,T)\cdot\left(F+1-M_{\mathrm{Ar}}(t,T)\right) \tag{14}$$

$$k^{1}_{\mathrm{ML}}(T) = k_1(T) \quad \text{and} \quad k^{2}_{\mathrm{ML}}(T) = k_2(T)\cdot A(0) \quad \text{and} \quad F = \frac{M_{\mathrm{B}}(0)}{M_{\mathrm{A}}(0)}\cdot\frac{m_{\mathrm{A}}}{m_{\mathrm{B}}} \tag{15}$$

$$M_{\mathrm{Ar}}(t,T) = \frac{k^{1}_{\mathrm{ML}}(T)+(F+1)\cdot k^{2}_{\mathrm{ML}}(T)}{k^{2}_{\mathrm{ML}}(T)+\left(k^{1}_{\mathrm{ML}}(T)+F\cdot k^{2}_{\mathrm{ML}}(T)\right)\cdot\exp\left(\left(k^{1}_{\mathrm{ML}}(T)+(F+1)\cdot k^{2}_{\mathrm{ML}}(T)\right)\cdot t\right)} \tag{16}$$

$$\mathrm{ML}(t,T) = OF_{\mathrm{ML}} + 100\%\cdot\frac{M(0)-M(t,T)}{M(0)} = OF_{\mathrm{ML}} + 100\%\cdot\left(1-M_{\mathrm{r}}(t,T)\right) \tag{17}$$

$$M_{\mathrm{r}}(t,T) = 1-\frac{m_{\mathrm{C}}}{m_{\mathrm{A}}}\cdot\frac{M_{\mathrm{A}}(0)}{M(0)}\left(1-M_{\mathrm{Ar}}(t,T)\right) \tag{18}$$

$$\mathrm{ML}(t,T) = OF_{\mathrm{ML}} + 100\%\cdot\frac{m_{\mathrm{C}}}{m_{\mathrm{A}}}\cdot\left(1-\frac{k^{1}_{\mathrm{ML}}(T)+k^{2}_{\mathrm{ML}}(T)}{k^{2}_{\mathrm{ML}}(T)+k^{1}_{\mathrm{ML}}(T)\cdot\exp\left(\left(k^{1}_{\mathrm{ML}}(T)+k^{2}_{\mathrm{ML}}(T)\right)\cdot t\right)}\right) \tag{19}$$

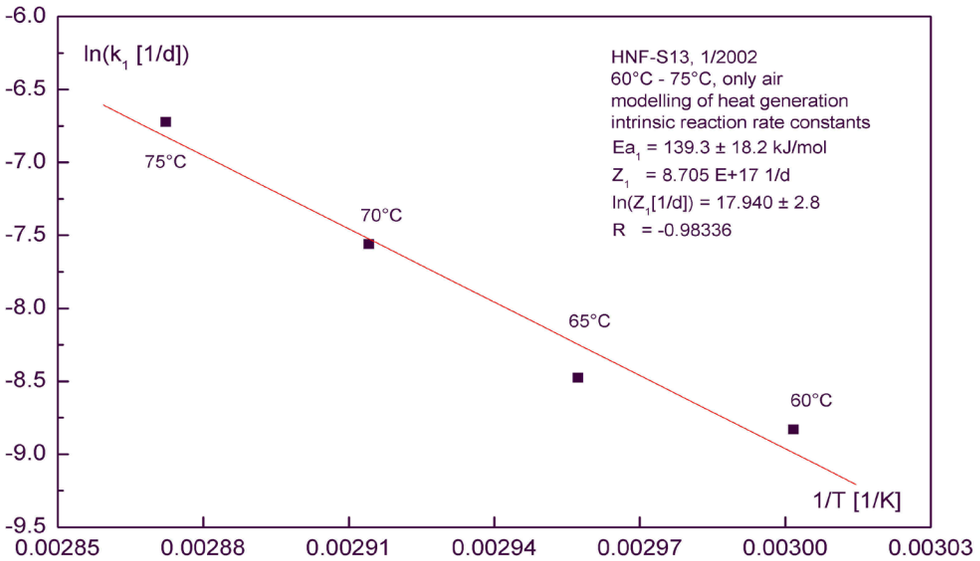

Figure 9. *HNF lot 2: Arrhenius plot of the reaction rate constant of the intrinsic decomposition of HNF, obtained by autocatalytic modelling of the heat generation.*

ML data of lot 1 and Figure 14 details the data for the lower temperatures. The strong autocatalytic decomposition of HNF can be seen in Figure 15. HNF decomposes nearly completely into gaseous products at 80 °C. But at lower temperatures it was also found that HNF decomposes nearly completely into gaseous products. From Figure 15 it is clear that the course of the complete decomposition of HNF is complicated. At least a two regime autocatalytic acceleration must be used to describe the complete decomposition. A self heating effect during the strong increase of mass loss may increase the decomposition rate additionally. Figure 16 shows the mass loss measurements up to 5% for HNF lot 2. The decomposition rate at 75 °C is somewhat higher with lot 2 than with lot

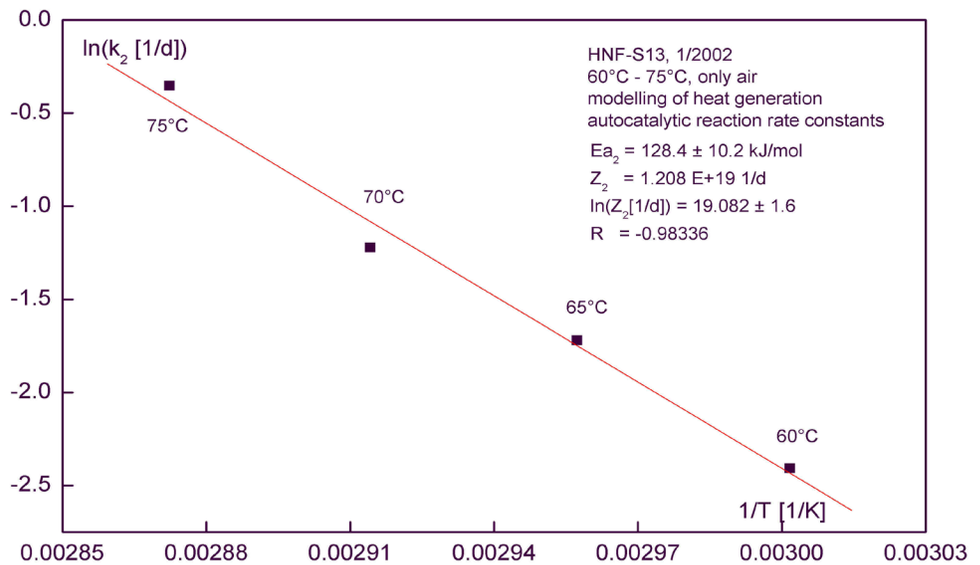

Figure 10. *HNF lot 2: Arrhenius plot of the reaction rate constant of the autocatalytic decomposition of HNF, obtained by autocatalytic modelling of the heat generation.*

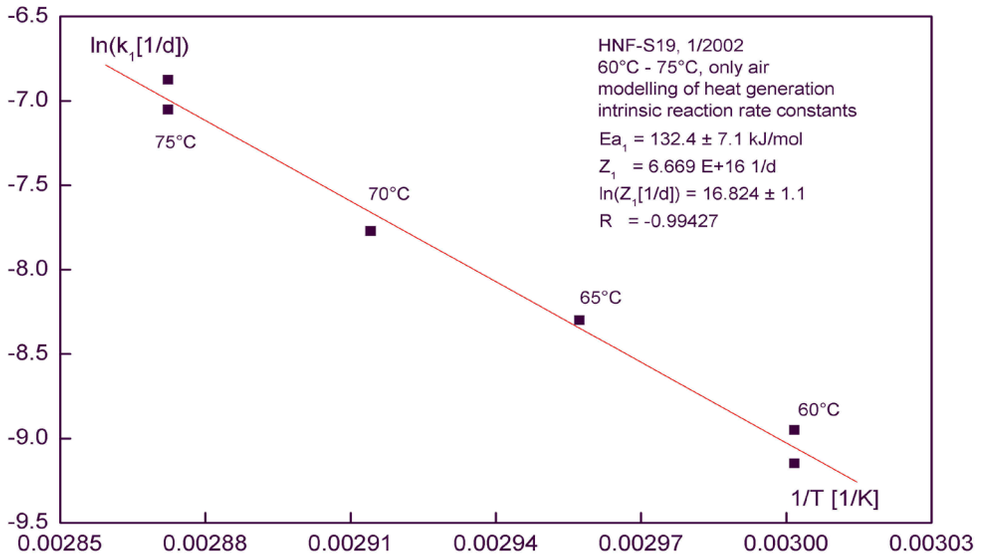

Figure 11. *HNF lot 3: Arrhenius plot of the reaction rate constant of the intrinsic decomposition of HNF, obtained by autocatalytic modelling of the heat generation.*

1. Figure 17 shows the mass loss measurements up to 5% for HNF lot 3. Here also the decomposition rate is higher for lot 3 than for lot 1, especially after an initial period. There lot 3 seems somewhat more stable.

Evaluation of mass loss data

The data evaluation was done with reaction kinetic modelling described in detail already elsewhere[9] and in short below. Here also the reaction scheme equation (4) with the corresponding rate equation, equation (5), is used. Equation (5) is converted to the description with masses whereby $M_{Ar}(t)=M_A(t)/M_A(0)$. The result is equation (14) with the reaction rate constants and F given in equation (15). The integration of equation (14) yields equation (16),

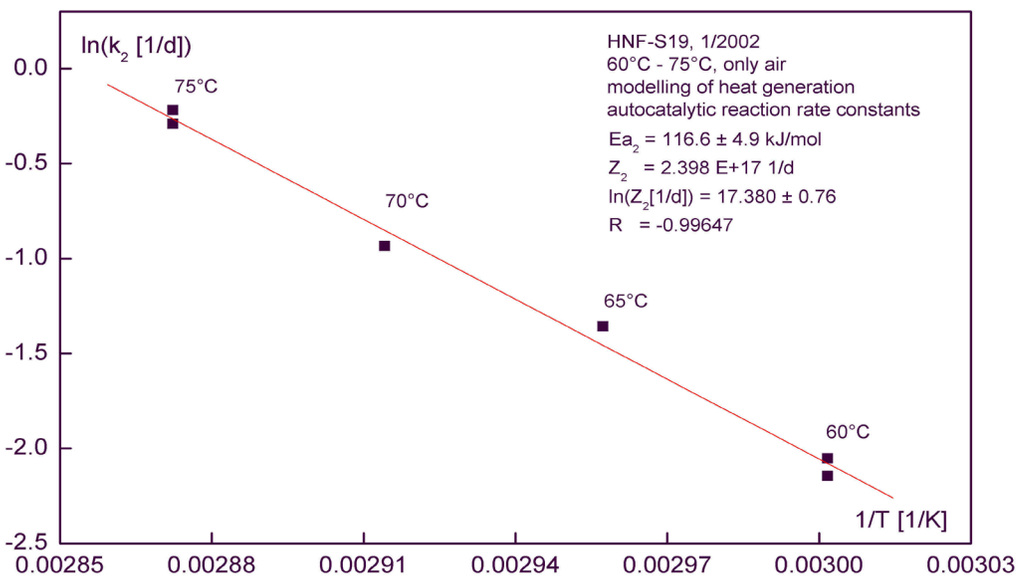

Figure 12. *HNF lot 3: Arrhenius plot of the reaction rate constant of the autocatalytic decomposition of HNF, obtained by autocatalytic modelling of the heat generation.*

$$t_{y_{ML}}(T) = t_{y_M}(T) = \frac{1}{k^1_{ML}(T) + k^2_{ML}(T)} \cdot \ln\left(\frac{\frac{1}{y_M} \cdot \left(k^1_{ML}(T) + k^2_{ML}(T) \right) - k^2_{ML}(T)}{k^1_{ML}(T)} \right) \tag{20}$$

$$y_M = \frac{M(t_{y_M}(T))}{M(0)} = M_r(t_{y_M}(T)) = 1 - \frac{y_{ML}}{100\%} \tag{21}$$

which is used for the autocatalytic modelling of the mass loss data. Because HNF decomposes nearly without residue, the summarized molar mass m_C of the gaseous species equals the molar mass m_A of the decomposing substance A, which is here HNF. With freshly prepared substances one may assume $F = 0$. Equation (17) stands for the actually measured mass loss and the normalized mass $M_r(t,T)$ is given by equation (18), which shows the connection of mass loss $M_{Ar}(t,T)$ of investigated substance A with the measured quantity $M_r(t,T)$. Together with the assumptions about m_C/m_A and F equation (19) results, which was used for the kinetic description of the measured data. The quantity OFML represents an offset not caused by decomposition of substance A. Figure 18 shows an example of the data modelling. Equation (20) is analogous to equation (12) to calculate the times t_{yML} to reach preset mass losses ML in the autocatalytic decomposition case. Equation (21) gives the relation between degree of mass change y_M and mass loss ML and y_{ML}.

As said above HNF shows a complicated decomposition course. But for the assessment of the in-service time (often named ‘lifetime’) of HNF the decomposition up to 5% ML is enough, because the performance data are after 5% out of tolerance already. During this decomposition range the curve is 'homogeneous' which means the reaction scheme of equation (4) is applicable, which is sustained by the good description of the data, see Figures 18a and 18b. The reaction rate constants of the intrinsic and autocatalytic

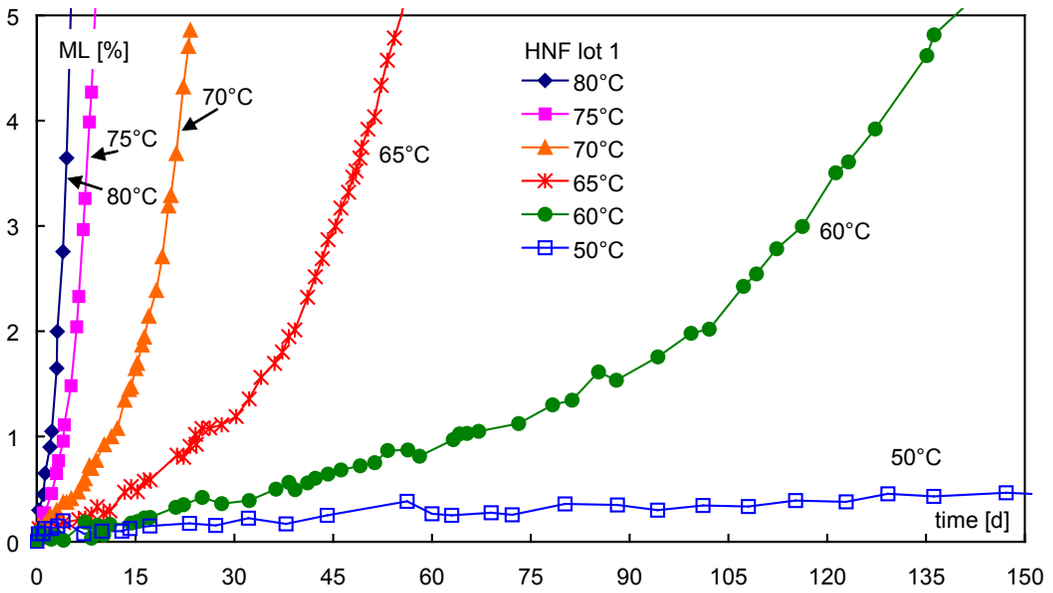

Figure 13. *HNF lot 1: Mass loss as function of time at the temperatures 50 °C, 60 °C, 65 °C, 70 °C, 75 °C and 80 °C.*

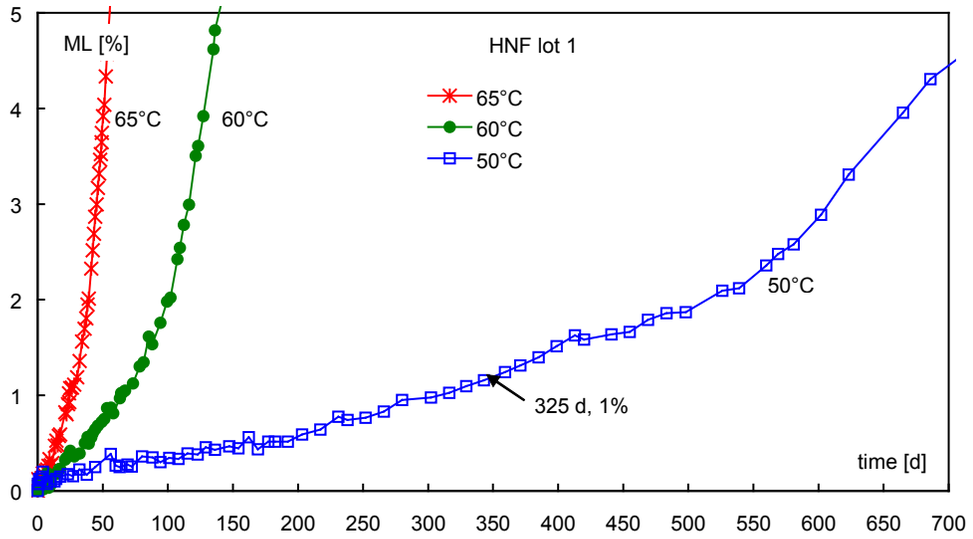

Figure 14. *HNF lot 1: Same as Figure 13, but coordinate scaling adapted to the curves at 50 °C, 60 °C and 65 °C.*

reaction are compiled in Table 8. There also the determined Arrhenius parameters of these two rate constants are given. The description of the data is always very good, recognizable with the high correlation coefficients. The Figures 19 and 20 show the Arrhenius plots of the two reaction rate constants. In Table 9 the times to reach preset mass loss values are given for the measurement temperatures, calculated with the reaction rate constants via equation (20). The times $t_{yML}(T)$ can be determined by calculation of the two rate constants via their Arrhenius parameters.

Discussion

Comparison of the three HNF lots

Table 10 shows all Arrhenius parameters obtained by reaction kinetic modelling. The activation energies from heat generation data are somewhat

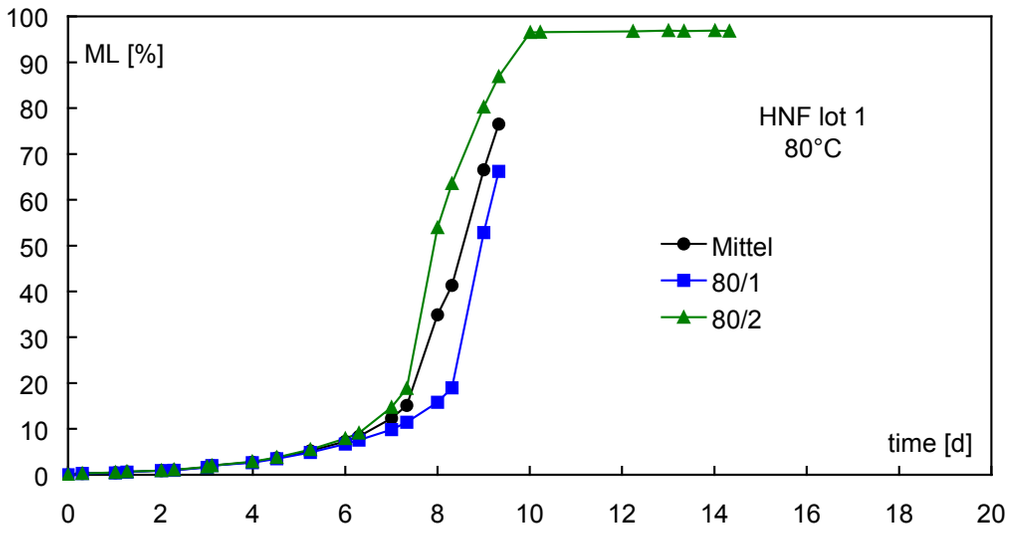

Figure 15. *HNF lot 1: Mass loss at 80 °C up to complete decomposition. HNF forms only a very small residue in slow thermal decomposition.*

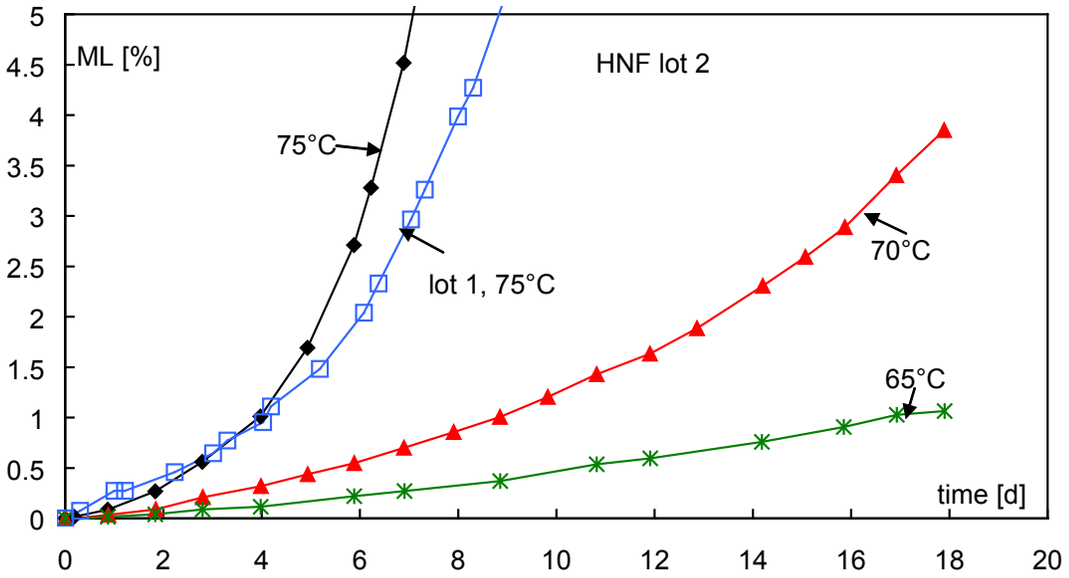

Figure 16. *HNF lot 2: Mass loss at 65 °C, 70 °C and 75 °C, compared with lot 1 at 75 °C.*

smaller than from mass loss. The interpretation could be that with HNF the two types of probing the decomposition reactions do not go in parallel as found with other systems.[8] The activation energies of HNF lot 2 and HNF lot 3 are on average somewhat different, but the values are within the error margins in congruence. In Tables 11 and 12 some characteristic data of the decomposition behaviour are listed, all at 75 °C.

The initial mass loss rates and energy loss rates differ from substance to substance. HNF lot 3 has the lowest initial rates. But in terms of mass loss it is the substance with the fastest decomposition rate, Table 13, followed by HNF lot 2 and then HNF lot 1.

In Table 14 the times to reach energy loss (EL) data are presented. To reach the same conversion expressed as ML or as EL needs significantly

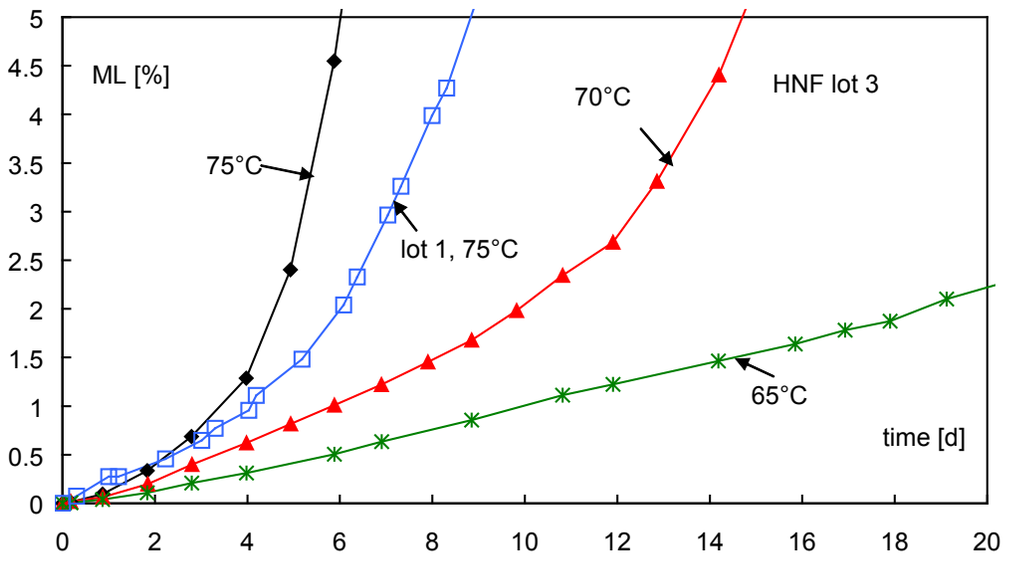

Figure 17. *HNF lot3: Mass loss at 65 °C, 70 °C and 75 °C, compared with lot 1 at 75 °C.*

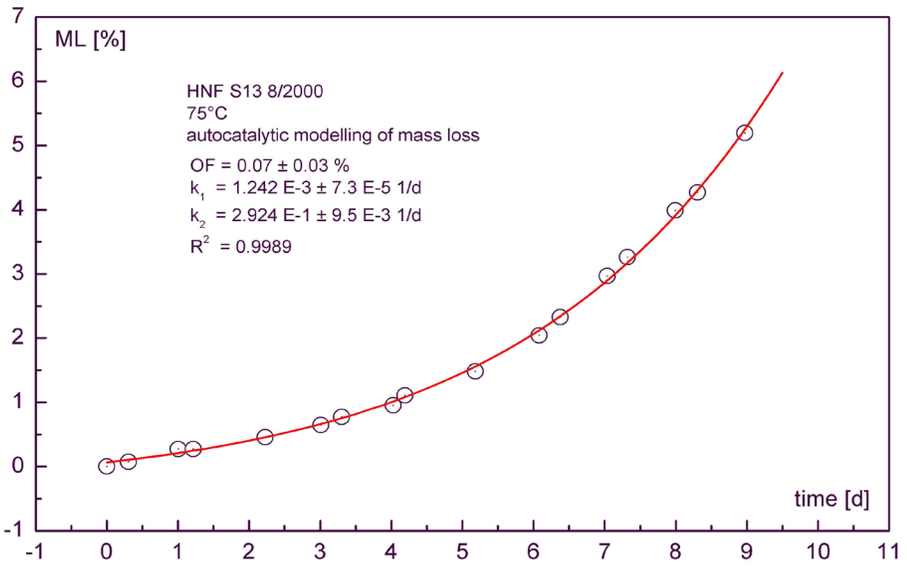

Figure 18a. *HNF lot 1: Autocatalytic modelling of the mass loss at 75 °C.*

less time as EL. This is surprising but confirms the above made assumption that the two criteria, evolution of gases and net sum of the heats of reaction, do not go in parallel with HNF. To solve this discrepancy a third method must be employed. The best is to follow the decomposition behaviour by detailed analysis of decomposition gases and of undecomposed HNF. Figure 21 shows the times t_{yEL} to preset energy losses for lots 2 and 3. To reach 1% EL at 30 °C needs about 4.2 years for lot 3 and 7.4 years for lot 2, see Table 15. In Figure 22 the comparison of the two kinetic descriptions can be seen. It shows the times to 1% EL with autocatalytic description and only first order description. The times of the first order description are longer by a temperature dependent factor between 3.1 and 4.5.

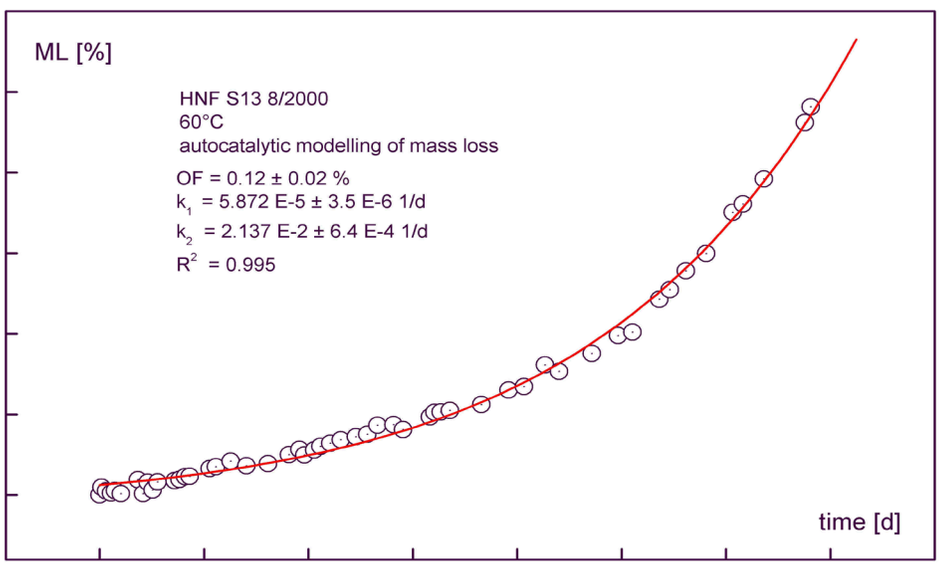

Figure 18b. *HNF lot 1: Autocatalytic modelling of the mass loss at 60 °C.*

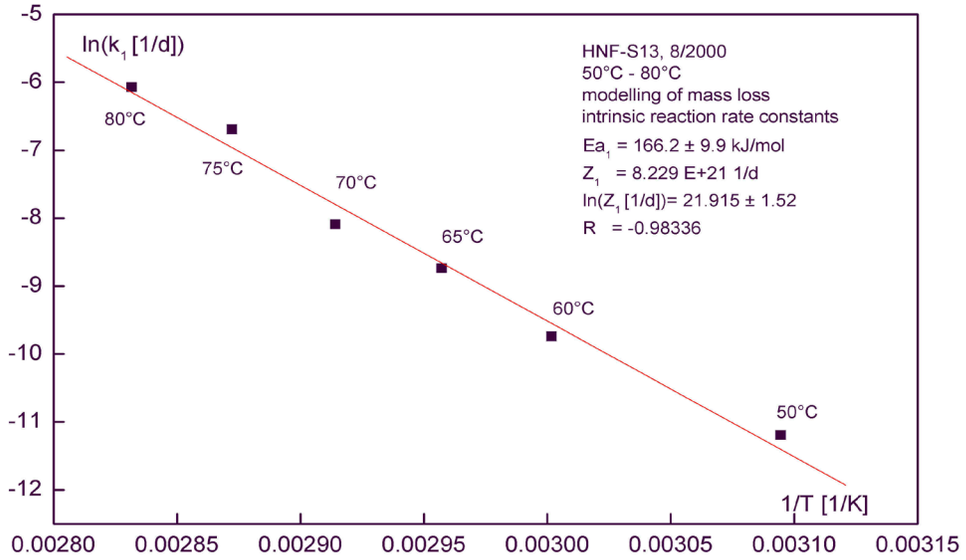

Figure 19. *HNF lot 1: Arrhenius plot of the reaction rate constant of the intrinsic decomposition of HNF, obtained by autocatalytic modelling of the mass loss.*

Comparison of HNF with other energetic material

In order to assess HNF as a possible ingredient in rocket propellants for military use, it is useful to compare it with other ingredients. Figure 23 compares the mass loss behaviour of HNF with that of unstabilized nitrocellulose (NC). This standard material with nitrogen content of 13.15% shows better stability than HNF. The adiabatic self heat rate, Figure 24, provides a similar insight. HNF is, in the series HNF < ADN < NC < CL20 < RDX < HMX, the most unstable substance. In comparison with ADN at lower temperatures HNF is less stable than ADN, see Figure 25, which compares the mass loss curves of HNF lot 1 and ADN ICT

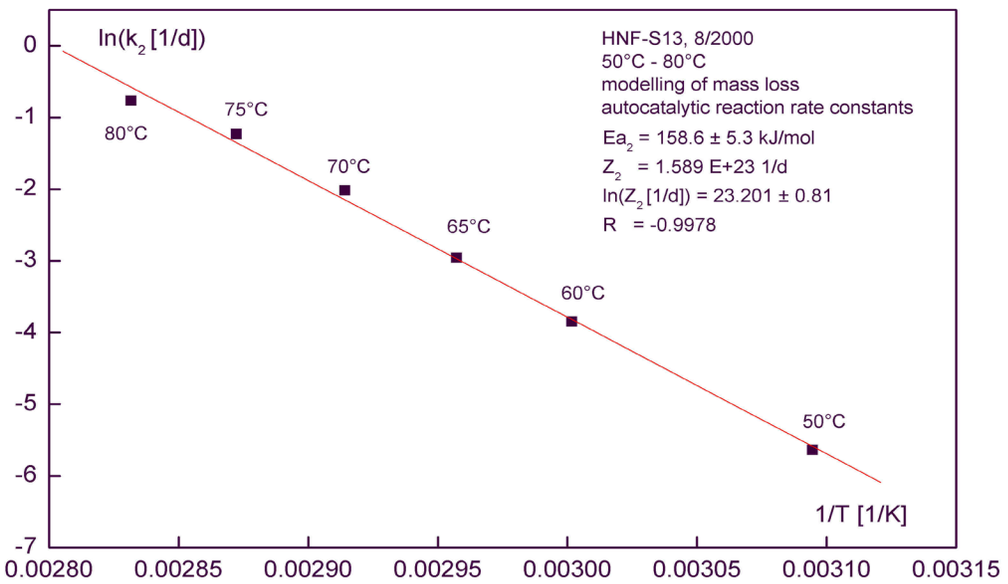

Figure 20. *HNF lot 1: Arrhenius plot of the reaction rate constant of the autocatalytic decomposition of HNF, obtained by autocatalytic modelling of the mass loss.*

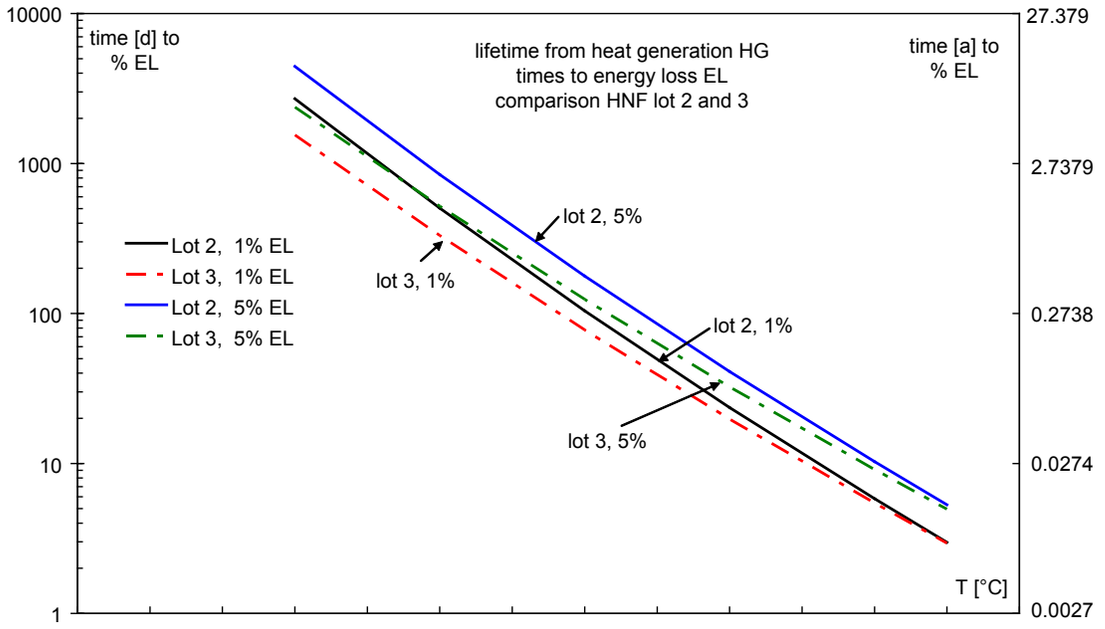

Figure 21. *Times tyEL to reach preset energy losses EL determined from the measured heat generation data of HNF lot 2 and 3.*

at 70 °C and 75 °C. It is to be noticed that the so-called anomalous decomposition behaviour of ADN at around 60 °C only appears at special conditions of ADN purity. In particular, the water content seems to have an important effect.[10] In most cases these conditions are not encountered with ADN in practice and in use one can adjust the water content in such a way that the anomalous decomposition of ADN will not be effective.

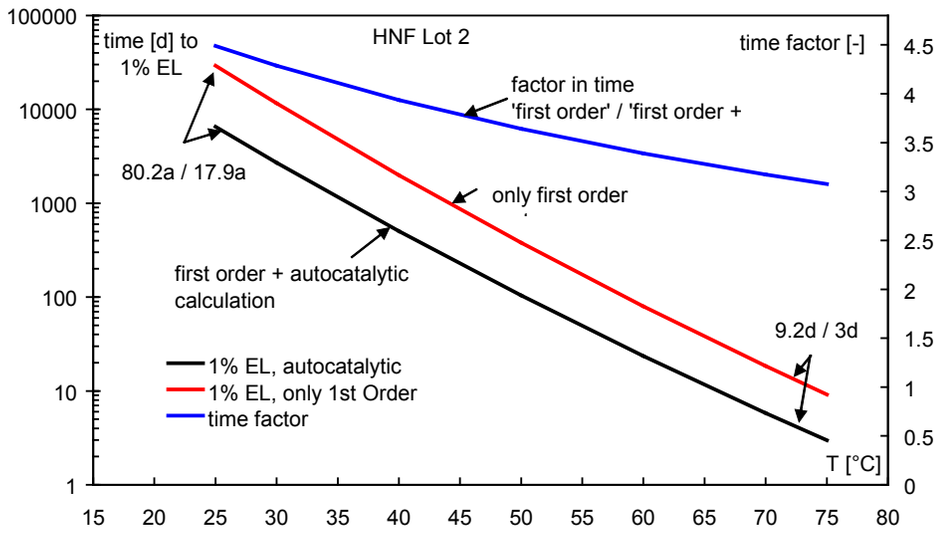

Figure 22. *Comparison of times t_{yEL} to reach preset energy loss EL determined with the autocatalytic model and with the reaction of first order only. The times determined by the last description are longer by a factor of about 3.1 to 4.5, depending temperature.*

Table 8. *HNF lot 1: Reaction rate constants obtained from autocatalytic modelling of mass loss up to 5%. The offset found equals in average nearly to the water content found at ICT, namely 0.18 mass%.*

Temp./°C	$k_{ML,1}$ [1/d]	$k_{ML,2}$ [1/d]	Offset [%]	R^2
80	$2.3120 \times 10^{-3} \pm 2.8 \times 10^{-4}$	$4.6470 \times 10^{-1} \pm 3.4 \times 10^{-2}$	0.19 ± 0.07	0.997
75	$1.2420 \times 10^{-3} \pm 7.3 \times 10^{-5}$	$2.9240 \times 10^{-1} \pm 9.5 \times 10^{-3}$	0.07 ± 0.03	0.999
70	$3.0670 \times 10^{-4} \pm 1.1 \times 10^{-5}$	$1.3300 \times 10^{-1} \pm 2. \times 10^{-3}$	0.18 ± 0.03	0.999
65	$1.6060 \times 10^{-4} \pm 6.8 \times 10^{-6}$	$5.1900 \times 10^{-2} \pm 1.1 \times 10^{-3}$	0.11 ± 0.02	0.998
60	$5.8720 \times 10^{-5} \pm 3.5 \times 10^{-6}$	$2.1370 \times 10^{-2} \pm 6.4 \times 10^{-4}$	0.12 ± 0.02	0.995
50	$1.3778 \times 10^{-5} \pm 7.5 \times 10^{-7}$	$3.5627 \times 10^{-3} \pm 1.2 \times 10^{-4}$	0.17 ± 0.02	0.992
Arrhenius parameters				
E_{ai}/kJ mol^{-1}	166.2 ± 10	158.6 ± 5		
lg(Z_i [1/d])	21.92 ± 1.5	23.20 ± 0.8		
R^2_i	0.993	0.998		

Table 9. *Times in days to reach preset ML at different temperatures for HNF lot 1, calculated with the corresponding reaction rate constants obtained by autocatalytic modelling, using equ\tion (19) and equ\tion (20). The offset, caused by residual water not included.*

ML [%]	50 °C [d]	60 °C [d]	65 °C [d]	70 °C[d]	75 °C [d]	80 °C [d]
1	360	72.1	27.9	12.65	4.15	2.38
2	514	99.6	39.0	17.16	6.00	3.50
3	615	117.1	46.1	20.03	7.21	4.24
5	751	140.3	55.6	23.80	8.85	5.26

Table 10. *Arrhenius parameters compiled for overview.*

HNF lot	Atmosphere	Type	Temp. range/°C	E_{a1}/ kJ mol^{-1}	lg(Z_1 [1/d])	R^2_1	E_{a2}/ kJ mol^{-1}	lg(Z_2 [1/d])	R^2_2
lot 1	air	ML	50–80	166.2 ± 10	21.92 ± 1.5	0.993	158.6 ± 5	23.20 ± 0.8	0.998
lot 2	air	HG	60–75	139.3 ± 18	17.94 ± 2.8	0.983	128.4 ± 10	19.08 ± 1.6	0.994
lot 3	air	HG	60–75	132.4 ± 7	16.82 ± 1.1	0.994	116.6 ± 5	17.38 ± 0.8	0.997

Table 11. *Characteristic decomposition data at 75 °C from mass loss. MLR means mass loss rate.*

HNF lot	Initial MLR at 75°C [%/d]	Intrinsic reaction rate constant $k_{ML}{}^1$ at 75 °C [1/d]	Autocatalytic reaction rate constant $k_{ML}{}^2$ at 75 °C [1/d]
HNF lot 1	0.124	1.242×10^{-3}	2.924×10^{-1}
HNF lot 2	0.081	8.115×10^{-4}	4.914×10^{-1}
HNF lot 3	0.072	7.193×10^{-4}	6.418×10^{-1}

Comparison of obtained kinetic data with literature data

HNF was investigated years ago with regard to thermal stability and decomposition. Such literature will be taken here which deals with the determination of decomposition parameters. An early work is that of Koroban *et al*.[11] He investigated the thermal decomposition of HNF between 70 and 100 °C by gas generation and has determined kinetic parameters. Also Brill[14] has investigated HNF with the fast heating method (T-jump) together with FTIR analyses of decomposition gases in the range 130 to 400 °C. Further studies containing decomposition parameters are from

Table 12. *Characteristic decomposition data at 75 °C from heat generation, measured in air. HGR means heat generation rate, ELR means energy loss rate determined with $Q_{ref} = Q_{EX} = 5580\ J\ g^{-1}$.*

HNF lot	Initial HGR and ELR at 75 °C		Intrinsic reaction rate constant k_Q^1 at 75 °C [1/d]	Autocatalytic reaction rate constant k_Q^2 at 75 °C [1/d]
	[µW g^{-1}]	[%/d]		
HNF lot 1	70.32	0.109	1.089×10^{-3}	7.728×10^{-1}
HNF lot 2	74.08	0.115	1.147×10^{-3}	7.383×10^{-1}
HNF lot 3	61.30	0.095	9.492×10^{-4}	7.759×10^{-1}

Table 13*: Times in days to reach given mass loss ML values at 75 °C for the three HNF lots, calculated with reaction rate constants obtained by autocatalytic modelling. The offset is excluded.*

ML [%]	Lot 1 [d]	Lot 2 [d]	Lot 3 [d]
1	4.15	3.99	3.59
2	6.00	5.27	4.60
3	7.21	6.06	5.22
5	8.85	7.10	6.03
10	11.26	8.59	7.17

TNO[4,5], from FOI[12] and from Sinditskii *et al*. by flame front measurements.[15]

Figure 26 compares the ML data of this work with the gas generation data of Koroban.[11] The curves look very similar. Also with gas generation the clear autocatalytic behaviour was observed. In Figure 27 the evaluation of Koroban's data can be seen up to a conversion of 18%, whereby the total decomposition gas amount GG(t_e) was obtained from Figure 26, right side. The description of the GG data is very good. In Figure 28 the measurements of heat generation rate on HNF at 60 °C are compared. The left side shows data from this work, the right side from TNO,[4] using an HNF from APP. That lot shows higher HGR than the lots used in this work. The last comparison between measurements of the two laboratories

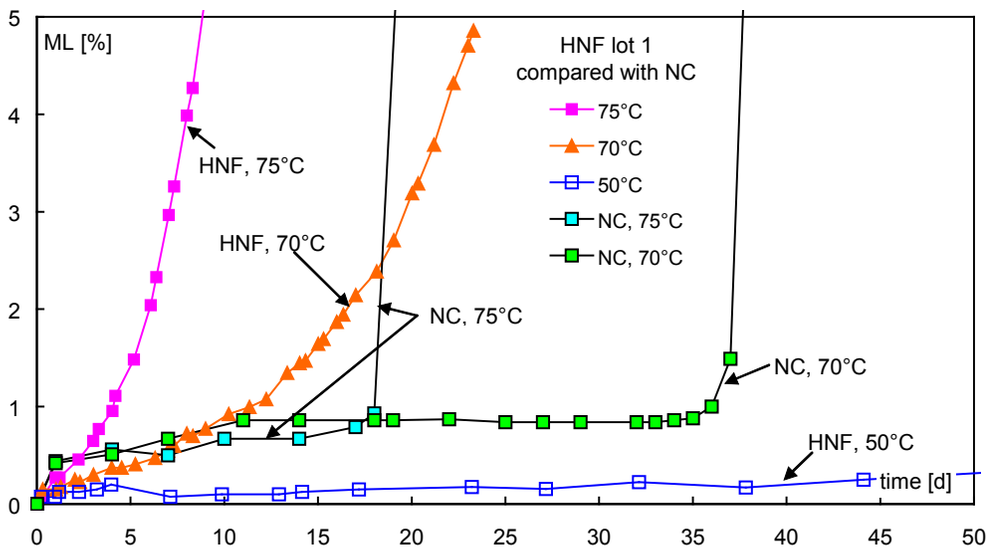

Figure 23. *Comparison between nitrocellulose (N content = 13.15%) and HNF lot 1 by mass loss measurements.*

Table 14. *Times in days to reach given energy loss EL values at 75 °C for the three HNF lots, calculated with reaction rate constants obtained by autocatalytic modelling.* $Q_{ref} = Q_{EX} = 5580\ J\ g^{-1}$. *Measurements in air.*

EL [%]	Lot 1 [d]	Lot 2 [d]	Lot 3 [d]
1	2.72	2.73	2.86
2	3.54	3.58	3.70
3	4.05	4.11	4.21
5	4.71	4.81	4.87
10	5.66	5.80	5.82

is made in Figure 29. Here also heat generation rates are compared obtained in this work and at FOI, Sweden.[12] The data are comparable; the HNF from FOI seems somewhat more stable than the lots used here.

Table 16 lists all Arrhenius parameters determined in this work and found in the cited literature. The data[5,14] are not in the range found from the other measurements. The parameters from gas generation[11] fit with data obtained from mass loss in the temperature range 50 to 80 °C. In the second last row of Table 16 autocatalytic description parameters are given, calculated from Figure 3, $C_0 * k_2$ in ref. 11, as was done for the initial first order decomposition. In the last row Koroban's data are given as cited in his paper[11] for the autocatalytic part. But for the first order or initial part this new set of E_{a1} and Z_1 was taken from Koroban's notes by Sinditskii and communicated to the author of this paper. The evaluated heat generation data of four lots are in agreement with each other within the limits of accuracy.

The parameters obtained from flame front measurements by Sinditskii[15] are a special case. The activation energy given in the row with E_a = 140.7 kJ mol^{-1} was calculated using equation (22) with data on TS and r_b(TS) obtained from Sinditskii. Equation (22) is an approximation for equation (23), which gives the results in the row below with E_a = 135.2 kJ mol^{-1}. These results, extractable from Sinditskii's data,[16] fit well with the determined data from heat generation. In

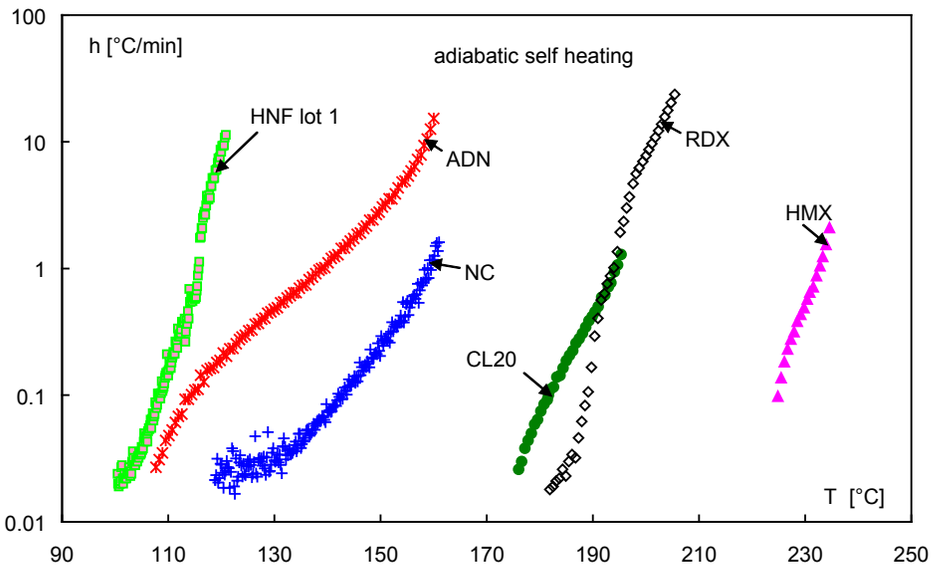

Figure 24. *Adiabatic self heat rate h as function of the adiabatically reached temperature of HNF, ADN, NC and some high explosives. Measurements performed with an ARC™. Sample mass between 200 mg and 300 mg.*

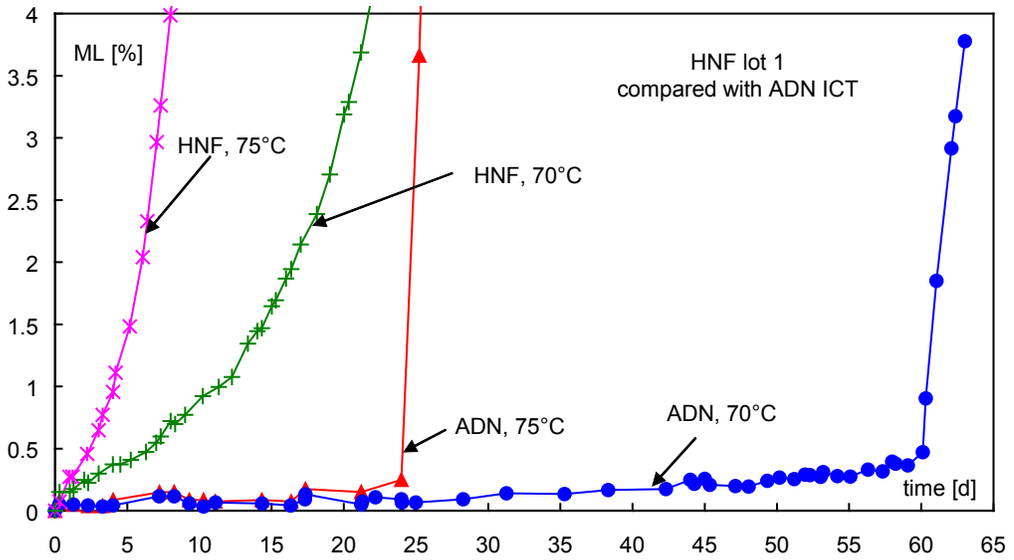

Figure 25. *Comparison by mass loss measurements of HNF lot 1 with un-stabilized ADN manufactured at ICT.*

equation (23) a lot of material properties are needed and data on the heat of reaction Q_R are often not easy to get. Information about the derivation of equation (23) can be found for example around equation (11).[17]

Certainly the activation energy E_a is often a complex quantity, especially the one determined from HGR or HG. But when the measurement method and the evaluation procedure have enough 'resolution' to separate the individual kinetic processes one can identify the activation energy of the limiting decomposition step of the material. Here one could assume that in the hot surface of the burning strand the activation energy found is assigned to the gasification process. This means one has with such methods high material conversion in the solid layer. The resulting description by Arrhenius parameters gives for E_a a mix of intrinsic first order reaction and the autocatalytic reaction. Then the apparent Arrhenius parameters derived from formal first order description as made by Brill and Sinditskii are composed of those of the individual reaction parameters. A sort of average is obtained. This can be seen if one uses the reciprocal times to reach a certain conversion (calculated with equation (12) for EL and equation (20) for ML) as

Table 15. *Times t_{yEL} to reach preset energy losses EL for HNF lot 2 and 3.*

	1% EL				3% EL				5% EL			
T/°C	Lot 2		Lot 3		Lot 2		Lot 3		Lot 2		Lot 3	
	[d]	[a]	[d]	[a]	[d]	[a]	[d]	[a]	[d]	[a]	[d]	[a]
20		44.4		21.9		62.8		29.4		71.7		32.9
25		17.9		9.51		25.4		12.8		29.1		14.4
30		7.40		4.24		10.6		5.76		12.2		6.50
40		1.38		0.91		2.00		1.25		2.31		1.42
50		0.28		0.21		0.42		0.30		0.48		0.34
60	23.6		19.8		35.2		28.3		40.9		32.4	
70	5.82		5.45		8.8		7.91		10.29		9.12	
75	2.98		2.94		4.53		4.3		5.31		4.97	
80	1.55		1.61		2.38		2.37		2.79		2.75	

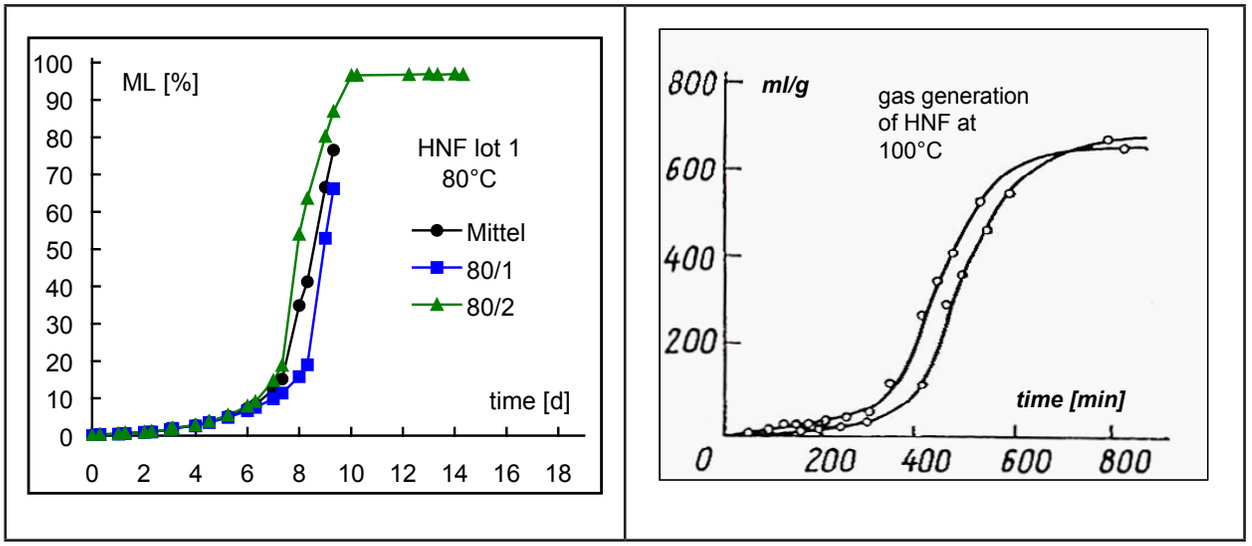

Figure 26. *Comparison of experimental data obtained for mass loss at 80 °C, this work, and on the right gas generation at 100 °C, figure taken from Koroban.*[11]

rate constants and determines from them the formal first order Arrhenius parameters. The apparent E_a has then values between E_{a1} and E_{a2}, the actual value depending on conversion. This is shown with data in Table 17 and their graphical representation in Figure 30. If a broader temperature range is used for the calculation of t_y then the process with greater activation energy is somewhat pronounced and the determined formal first order E_{aty} values are a bit greater, as can be seen in Table 17.

An instructive comparison of Arrhenius parameters is achieved by plotting the corresponding reaction rate constants together as in Figures 31 to 33 for the first order and the autocatalytic rate constants. From Figure 31 one recognizes that the Arrhenius parameters of Brill and de Klerk deviate significantly from the others. The Arrhenius parameters of Sinditskii correspond well with those obtained from heat generation data, but the correlation with mass loss and gas generation derived values is still acceptable. Figure 32 shows only the first order rate constants from autocatalytic descriptions. Gas generation and mass loss correspond very well and also the

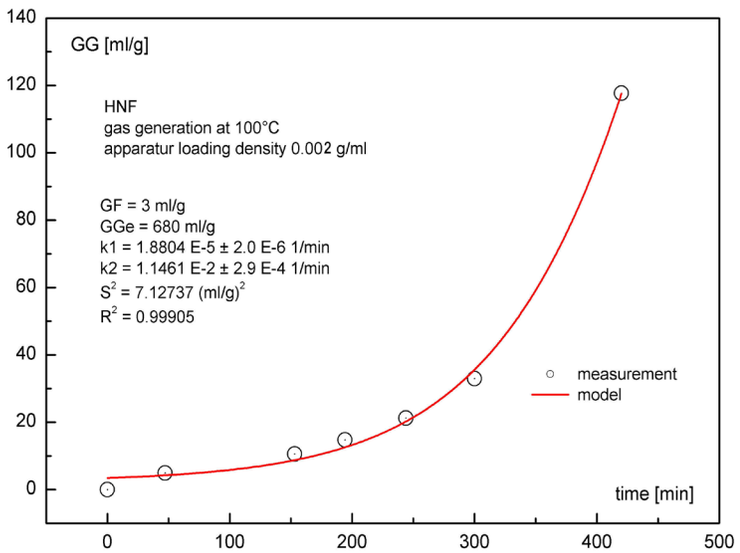

Figure 27. *Modelling of the data*[11] *with the autocatalytic model.*

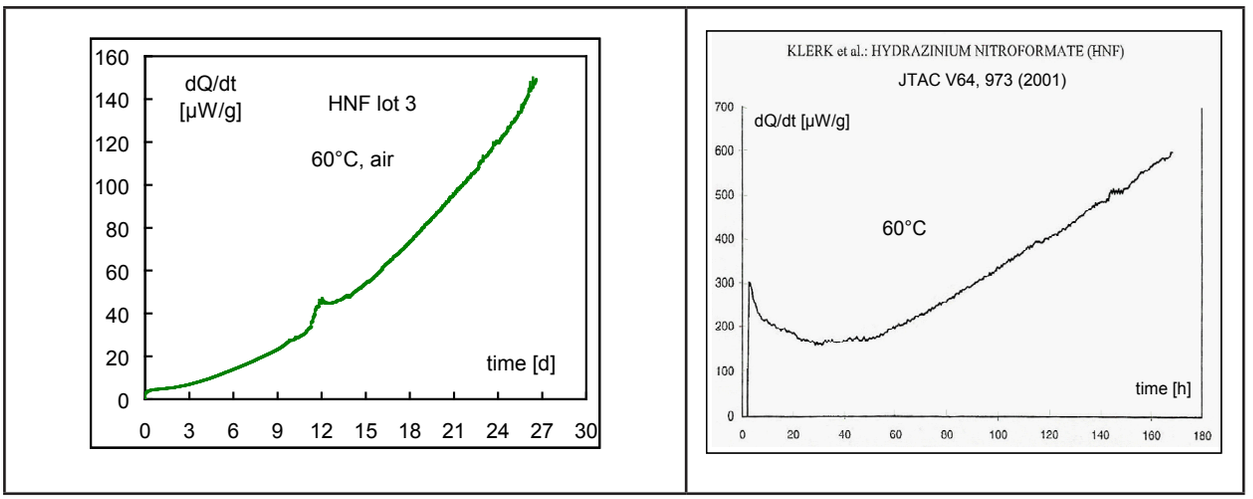

Figure 28. *Comparison of heat generation rates measured with HNF at 60 °C, on the left this work, and on the right figure taken from W. de Klerk.*[4]

HG derived data are in good agreement. Only FOI-E8 deviates somewhat because of a somewhat small pre-exponential factor. In Figure 33 the rate constants k_2 from the autocatalytic part can be seen. Again gas generation and mass loss correspond well and the group of HG derived values also. For both cases, k_1 and k_2, there is a certain difference between the group of HG data and the data group from mass loss and gas generation data. The reason may be the different loading densities applied. Table 18 lists the situation for the measurements of this work. With mass loss the loading density was relatively small with about 0.08 g cm^{-3} for the most measurements. Additionally one has some escaping of decomposition gases due to the nature of the method. In HGR measurements one has sealed ampoules and the average of loading density was about 0.43 g cm^{-3} and for the 60 °C measurements some 0.68 g cm^{-3}. The loading density during ML measurements is nominally only 18% of that of HG measurements, and it may be accounted smaller because of the not really sealed ML vials. Koroban[11] reports a remarkable dependence of HNF decomposition behaviour

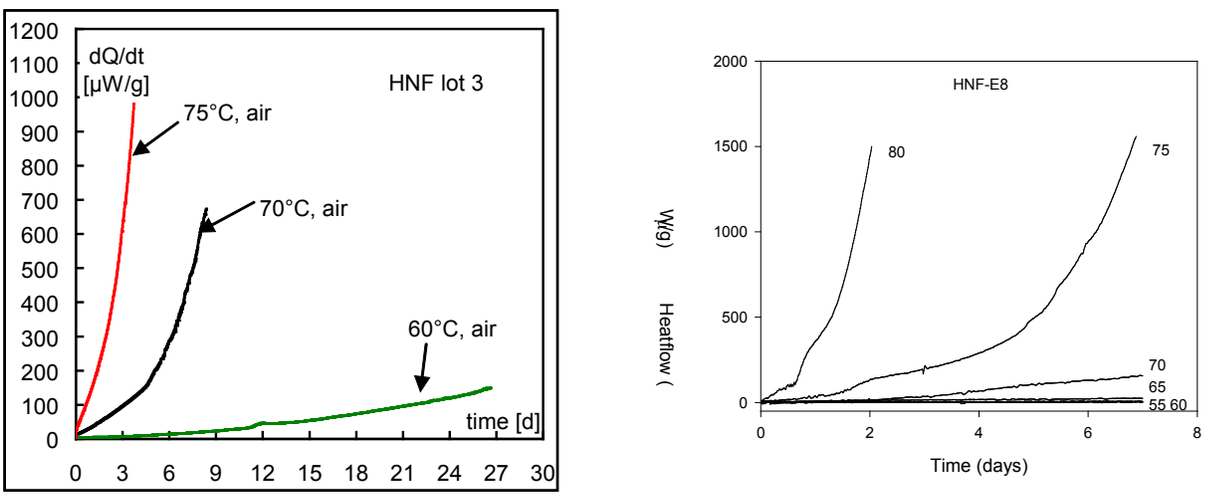

Figure 29. *Comparison of heat generation rates measured with HNF at several temperatures, on the left this work, and on the right measurements from FOI, Grindsjön Research Center, Tumba, Sweden,*[12] *used with permission.*

$$r_b(T_S) = Z_{rb}(T_S) \cdot \exp\left(-\frac{Ea_{Qr}}{2 \cdot R \cdot T_S}\right) = \sqrt{F(T_S) \cdot Z_{Qr} \cdot \exp(-Ea_{Qr} / RT_S)} = \sqrt{F(T_S) \cdot k_{Qr}(T_S)} \quad (22)$$

$$r_b(T_S) = \frac{\sqrt{Z_{Qr} \cdot \exp(-Ea_{Qr} / RT_s) \cdot 2 \cdot \rho \cdot \lambda \cdot Q_r \cdot \frac{RT_s^2}{Ea_{Qr}}}}{\rho \cdot c_p \cdot (T_s - T_0 + L_m / c_p)} = \frac{\sqrt{2\rho\lambda \cdot Q_r \cdot \frac{RT_s^2}{Ea_{Qr}} \cdot \sqrt{Z_{Qr}}}}{\rho \cdot c_p \cdot (T_s - T_0 + L_m / c_p)} \cdot \exp\left(-\frac{Ea_{Qr}}{2 \cdot RT_s}\right) \quad (23)$$

r_b	linear burning rate of strand
k_{Qr}	reaction rate constant for heat release in solid phase at combustion
Z_{rb}	pre-exponential factor for burning rate (with weak dependence on T_S)
E_{aQr}	activation energy for decomposition, heat release in solid phase at combustion
Z_{Qr}	pre-exponential factor for decomposition, heat release in solid phase at comb.
F	proportionality factor, depended on material properties and weakly on T_S
T_S	surface temperature of strand (can be measured by micro thermocouples)
T_0	strand temperature not heated
Q_r	heat of decomposition reaction
ρ	mass density
λ	heat conductivity
c_P	specific heat
L_m	heat of melting
R	general gas constant

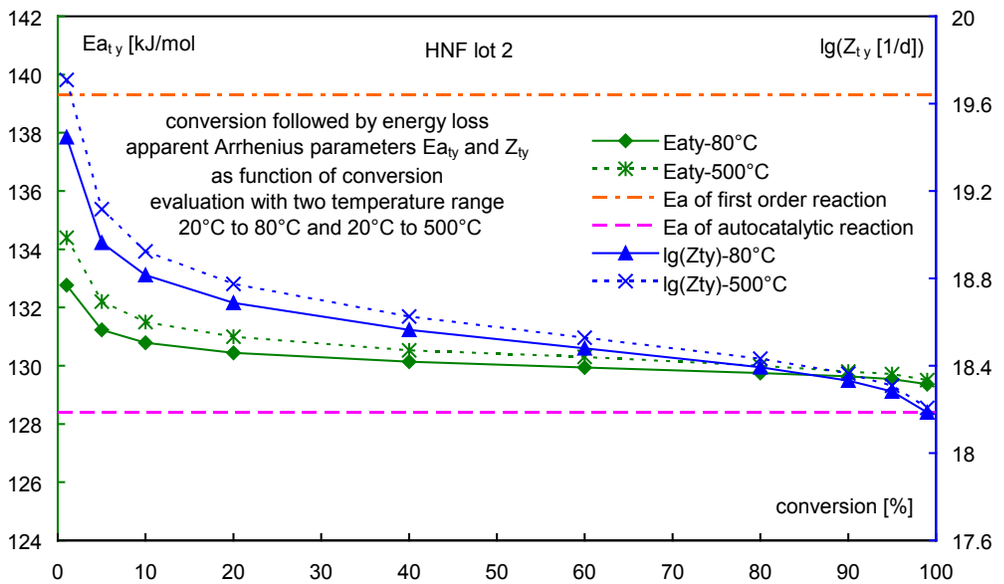

Figure 30. *Apparent Arrhenius parameters are obtained if one does not resolve the underlying reactions. Here with the real Arrhenius parameters of autocatalytic description the times t_{yEL} have been calculated as function of temperature up to given conversions. The temperature dependence of these times can formally be described with on set of Arrhenius parameters E_{aty} and Z_{ty}. These two parameters are a mix of the underlying parameters obtained by autocatalytic description.*

Table 16. *Compilation of Arrhenius data obtained for HNF from this work (APP type S) and from literature.*

Lot	Data type	Temp. range [°C]	Description with model 'Q: first order + autocatalytic'					
			E_{a1}/kJ mol^{-1}	lg(Z_1 [1/d])	R^2_1	E_{a2}/kJ mol $\times 10^{-1}$	lg(Z_2 [1/d])	R^2_2
HNF 1	Mass loss	50–80	166.2 ± 10	21.92 ± 1.5	0.993	158.6 ± 5	23.20 ± 0.8	0.998
HNF 2	Heat generation	60–75	139.3 ± 18	17.94 ± 2.8	0.983	128.4 ± 10	19.08 ± 1.6	0.994
HNF 3	Heat generation	60–75	132.4 ± 7	16.82 ± 1.1	0.994	116.6 ± 5	17.38 ± 0.8	0.997
Description with kinetics of 'first order' or of single step								
	Mass loss, TGA	100–150	226.5 ± 17	26.37 ± 2.3	(0.97) ?	de Klerk *et al*., 2003[5]		
	Gas generation	70–100	176.6 ± 21	23.50 ± 3.1	0.972	Koroban *et al*., 1979[11] lg(Z_1 [ml g^{-1} d^{-1}])= 26.33 ± 3.1 for initial decomposition only		
	T-jump, using induction time	130–140	105 ± ?	15.97 ± ?	?	Williams, Brill, 1995[14] pre-exp. factor estimated		
	Flame front	292–477	140.7 ± 4.6	17.93 ± 0.41	0.957	Sinditskii *et al*., 2002[15] lg(Z_{rb} [mm s^{-1}]) = 5.95 ± 0.18		
	Flame front	292–477	135.2 ± 6.8	17.59 ± 0.47	0.956	Sinditskii, 2006,[16] equation (23)		
Following results based on personal communication.[13] HNF samples from APP, type C and E. Measurements from ref. 12. Data description with model '*Q*: first order + autocatalytic'								
E type	Heat generation	60–80	137.3 ± 6.6	17.11 ± 1.0	0.993	117.7 ± 10.6	17.61 ± 1.6	0.976
C type	Heat generation	60–80	134.0 ± 9.8	17.07 ± 1.5	0.979	118.2 ± 10	17.56 ± 1.6	0.971
Complete data from Koroban *et al*.,[11] recalculated from data given in Figure 3 in ref. 11, k_1/670 [ml g^{-1}] and C_0*k_2								
	Gas generation	70–100	176.6 ± 21	23.50 ± 3.1	0.972	135.0 ± 0.6	19.64 ± 0.1	0.9999
Data from Koroban *et al*.[11] and by personnel communication[16]								
	Gas generation	70–100	169.6 ± ?	22.59 ± ?	?	144.8 ± ?	21.04 ± ?	?

Table 17. *Apparent Arrhenius parameters obtained by calculation of times t_{yEL} as function of temperature to reach given conversions (energy losses) for HNF lot 2. First order E_{a1} = 139.3 kJ mol^{-1}, autocatalytic E_{a2} = 128.4 kJ mol^{-1}.*

Conversion by energy loss EL [%]	20 to 500 °C		20 to 80 °C	
	E_{aty} [kJ/mol]	lg(Z_{ty} [1/d])	E_{aty} [kJ mol^{-1}]	lg(Z_{ty} [1/d])
1	134.4	19.709	132.77	19.446
5	132.2	19.117	131.23	18.963
10	131.5	18.924	130.79	18.815
20	131.0	18.774	130.44	18.688
40	130.5	18.626	130.14	18.564
60	130.3	18.529	129.94	18.480
80	123.0	18.432	129.75	18.393
90	129.8	18.364	129.64	18.332
95	129.7	18.309	129.54	18.282
99	129.5	18.207	129.37	18.186

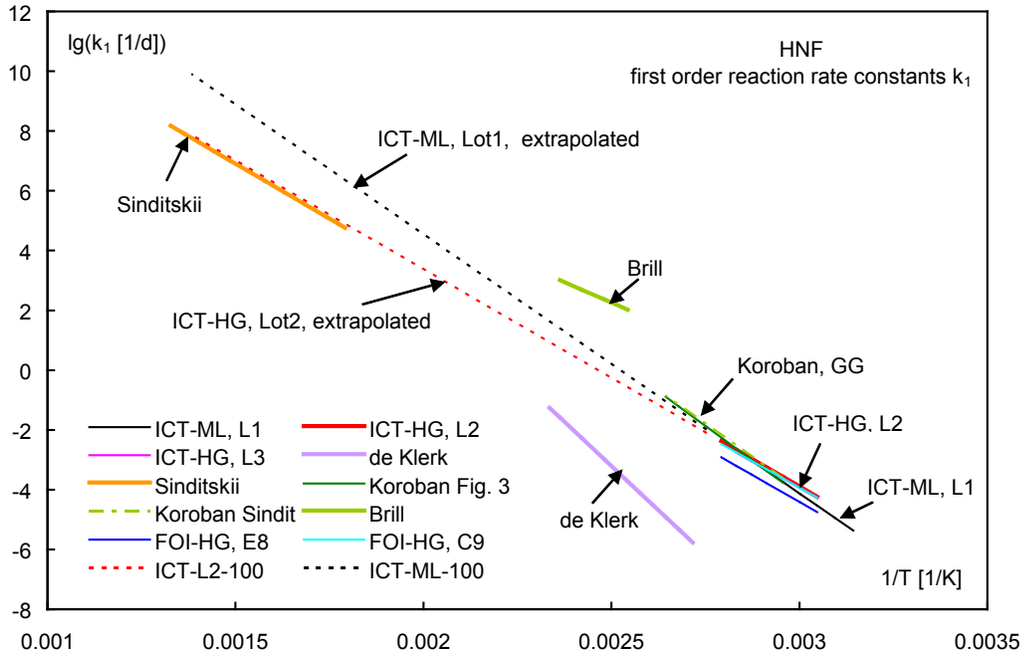

Figure 31. *Comparison of reaction rate constants k_1 of first order reaction in autocatalytic descriptions and apparent first order rate constants from other descriptions.*

on loading density. The differences found in the Arrhenius parameters of this work could originate in such a dependence on loading density. But also the probing itself of the two methods could result in differences. The two methods gas evolution and release of heat may see a different weighting of the ongoing complex decomposition processes and or may recognize different rate determining steps.

Conclusion

The thermal-chemical stability of the energetic substance HNF is such that it cannot be seen as non-handling substance. At room temperature it can be stored for several years as pure material. Substances like unstabilized NC and ADN have better stability behaviour than HNF. The determined relatively small values of activation energies, from mass loss (lot 1) data 166 kJ mol^{-1} and with heat generation between 132 and 140 kJ mol^{-1} for lots 2 and 3, each for the intrinsic decomposition reaction, reflect the reduced thermal stability of HNF. HNF decomposes autocatalytically. The activation energies for this part are smaller than for the intrinsic decomposition. A comparative

Table 18. *Loading densities (LD) of the ML and HGR measurements. Mass loss was determined in vials with volume of 12.6 ml, closed by ground stoppers. The HGR were determined in glass ampoules closed with a rubber sealing, volume 3 ml. E means amount weighed in, free volume in vials and ampoules calculated for the situation at begin of the measurements with HNF density of 1.91 g cm^{-3}.*

Temp./ °C	ML, Lot 1			HGR, Lot 2			HGR, Lot 3		
	E/g	LD/ g cm^{-3}	Free vol./cm^3	*E*/g	LD/ g cm^{-3}	Free vol./cm^3	*E*/g	LD/ g cm^3	Free vol./cm^3
80	0.5	0.040	12.338						
75	1.0	0.079	12.076	1.29	0.430	2.325	1.30	0.433	2.319
70	1.0	0.079	12.076	1.30	0.433	2.319	1.25	0.417	2.346
65	1.0	0.079	12.076	1.28	0.427	2.330	1.28	0.427	2.330
60	1.0	0.079	12.076	1.93	0.643	1.990	2.14	0.713	1.880
50	1.0	0.079	12.076						

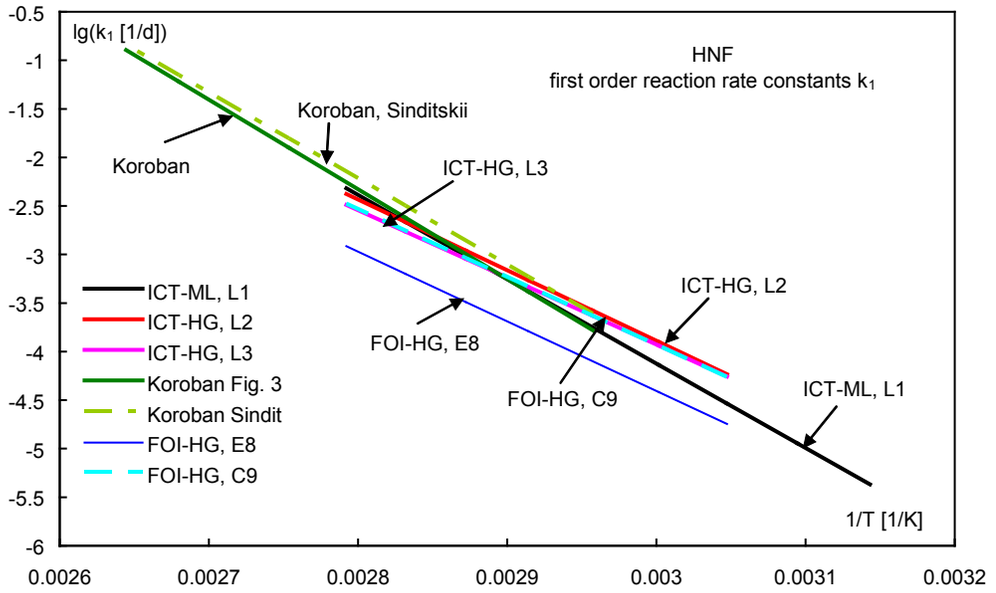

Figure 32. *First order reaction rate constants k_1 in autocatalytic descriptions only.*

discussion of the Arrhenius parameters found here and those which can be found in the literature shows a good agreement between the methods of the same probing type: this means agreement between mass loss and gas generation and between evaluations based on heat generation. Nevertheless the stability of HNF is such that it may be stored at 25 °C for several years until reaching a mass loss of 1%. The autocatalytic decomposition of HNF is not delayed as with nitrocellulose, it starts

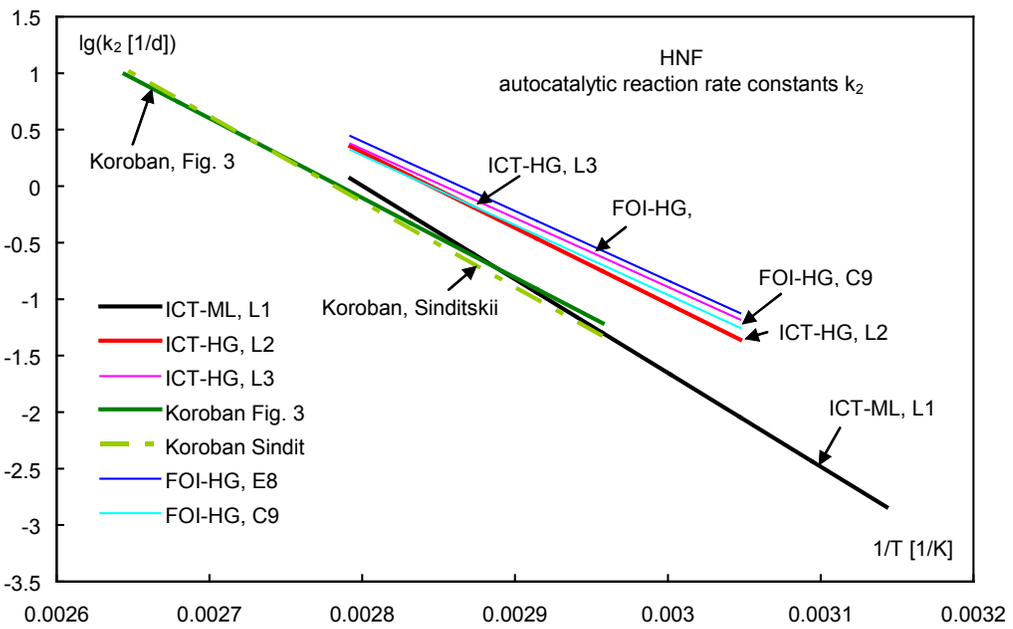

Figure 33. *Comparison of reaction rate constants k_2 of autocatalytic reactions in autocatalytic descriptions.*

from the beginning on. An additional source of risk is the high heat generation rate HNF is able to show. This limits non-stabilized HNF to handling only in containers of small geometric dimensions. The use in military ammunition with the demand to handle it up to 71 °C (highest environmental temperature according to STANAG 2895) does not seem advisable. The high heat generation rates during HNF decomposition would be a source of a non-manageable danger. Further to this the possibility of stabilizing HNF seems questionable. HNF decomposes via very reactive species, and probably they cannot be trapped fast enough by stabilizers added in the usual amounts.

Acknowledgements

Valuable discussions and the additional information about results from Koroban are acknowledged to Prof. V. P. Sinditskii, Mendeleev University of Chemical Technology, Moscow, Russia.

Dr Niklas Wingborg is thanked for providing of heat generation data measured at FOI, Grindsjön Research Center, Tumba, Sweden and using them in this publication.

Dr Antoine van der Heijden, TNO, The Netherlands, is thanked for discussions and for allowing the publication of the data presented in this work, which were obtained during a collaborative programme between TNO (PML at that time) and ICT Also thanked is Wim de Klerk for reproducing the right part of Figure 28, which was taken from his publication in the *Journal of Thermal Analysis and Calorimetry*, vol. 64, 2001, pp. 973–985.

List of abbreviations

HNF	hydrazinium nitroformate (older name also hydrazine trinitromethane)
ADN	ammonium dinitramide
NC	nitrocellulose
RDX	1,3,5-trinitro-1,3,5-triaaza-cyclohexane (Hexogen, Research Development eXplosive or Royal Demolition eXplosive)
CL20	China Lake explosive no. 20, laboratory short name of HNIW; 2,4,6,8,10,12-hexanitro-2,4,6,8,10,12-hexaaza-tetracyclo-[5.5.0.$0^{5,9}$.$0^{3,11}$]-dodecane
HMX	octogen, cyclo-tetramethylene-tetranitramine, or 1,3,5,7-tetranitro-1,3,5,7-tetraaza-cyclooctane(High Melting Explosive or Her Majesty's Explosive)
AP	ammonium perchlorate
AN	ammonium nitrate
ARC™	Accelerating Rate Calorimeter, determines adiabatic self heat rate
TAM™	Thermal Activity Monitor, microcalorimeter, determines heat generation rate
ML	mass loss
EL	energy loss
HGR	heat generation rate (dQ/dt)
HG	heat generation (Q)
GG	gas generation
VST	vacuum stability test
TGA	thermo gravimetric analysis
E_{aML}	activation energy from mass loss data
Z_{ML}	pre-exponential factor from mass loss data; $k_{ML} = Z_{ML} * \exp(-E_{aML}/RT)$
E_{aQ}	activation energy from heat generation or HGR data
Z_Q	pre-exponential factor from HG or HGR data; $k_Q = Z_Q * \exp(-E_{aQ}/RT)$
t_{yML}	time to reach a certain value of mass loss
t_{yEL}	time to reach a certain value of energy loss
Q_{EX}	heat of explosion

References

1 H. Bathelt, F. Volk and M. Weindel, The ICT Thermochemical Data Base, *Proceedings of the 30th International Annual Conference of ICT*, pp. 56-1 to 56-12, June 29–July 2, 1999, Karlsruhe, Germany. Fraunhofer-Institut für Chemische Technologie (ICT), Postfach 1240, D-76318 Pfinztal-Berghausen, Germany.

2 J. M. Bellerby, C. S. Blackman, P. Gill, W. H. M. Welland-Veltmans and A. E. D. M. van der Heijden, Decomposition of Hydrazinium Nitroformate (HNF) between 60°C and 80°C, *Proceedings of the 12th Symposium on 'Chemical Problems Connected with the Stability of Explosives'*, pp. 1 to 10, May 13–17, 2001, Karlsborg, Sweden, ed. Ola Listh, Combustion Institute of FOI, Stockholm 2004.

3 S. Löbbecke, H. Schuppler and W. Schweikert, Thermal Analysis of Hydrazinium Nitroformate (HNF), *Proceedings of the of the 32nd Annual Conference of ICT*, pp. 145-1 to 145-12, July 3–6, 2001, Karlsruhe, Germany. Fraunhofer-Institut für Chemische Technologie (ICT), D-76318 Pfinztal-Berghausen, Germany.

4 W. P. C. de Klerk, A. E. D. M. van der Heijden and W. H. M. Veltmans, Thermal Analysis of the High Energetic Material HNF, *Journal of Thermal Analysis and Calorimetry*, Vol. 64, 2001, pp. 973–985.

5 W. P. C. de Klerk, C. Popescu and A. E. D. M. van der Heijden, Study of Decomposition Kinetics of FOX-7 and HNF, *Journal of Thermal Analysis and Calorimetry*, Vol. 72, 2003, pp. 955–966.

6 HNF General data sheet, January 3, 2001, APP 1995-015, APP (Aerospace Propulsion Products BV), 4791 RT Klundert, NL,

7 HNF-Analysis sheet. APP (Aerospace Propulsion Products BV), 4791 RT Klundert, NL.

8 M. A. Bohn, Stability and Ageing Assessment of Rocket Propellant Formulation Batches with high Burn Rates, *Proceedings of the 3rd International Heat Flow Calorimetry Symposium for Energetic Materials*, pp. R1 to R15, April 8–11, 2002, French Lick, Indiana, USA.

9 M. A. Bohn, Kinetic Description of Mass Loss Data for the Assessment of Stability, Compatibility and Aging of Energetic Components and Formulations Exemplified with ε-CL20, *Propellants Explosives Pyrotechnics*, Vol. 27, 2002, pp. 125–135.

10 G. B. Manelis, G. M. Nazin, Yu. I. Rubtsov and V. A. Strunin, *Thermal Decomposition and Combustion of Explosives and Propellants*, Taylor & Francis, London and New York, 2003.

11 V. A. Koroban, T. I. Smirnova, T. N. Bashirova and B. S. Svetlov, Kinetics and mechanisms of thermal decomposition of hydrazine trinitromethane (in Russian), *Trudy Moskovskogo Khimiko-Tekhnologicheskogo Instituta imeni D.I. Mendeleeva (Proceedings of Mendeleev Institute of Chemical Technology)*,Vol. 104, 1979, pp. 38–44.

12 N. Wingborg and M. van Zelst, Comparative study of the properties of ADN and HNF. Report FOA-R--00-1423-310--SE. June 2000.

13 N. Wingborg, Swedish Defence Research Agency, FOI, Grindsjön Research Center, Tumba, Sweden.

14 G. K. Williams and T. B. Brill, Thermal Decomposition of Energetic Materials 67. Hydrazinium Nitroformate (HNF) Rates and Pathways under Combustion like Conditions, *Combustion and Flame*, Vol. 102, 1995, pp. 418–426.

15 V. P. Sinditskii, V. V. Serushkin, S. A. Filatov and V. Yu. Egorshev, Flame structure of hydrazinium nitroformate, *Proceedings of the 5th International Symposium on ' Special Topics in Chemical Propulsion (5-ISICP): Combustion of Energetic Materials'*, pp. 576 to 586, June 17 to 25, 2000, Stresa, Italy, Ed. K. K. Kuo and L. T. DeLucca, Begell House, Inc., New York, 2002.

16 Personal communication with V. P. Sinditskii, Mendeleev University of Chemical Technology, 9 Miusskaya Square, 125047, Moscow, Russia.

17 A. G. Merhanov and A. E. Averson, The Present State of the Thermal Ignition Theory. An Invited Review, *Combustion and Flame*, Vol. 16, 1971, pp. 89–124.